

# A new species of *Nanhsiungchelys* (Testudines: Cryptodira: Nanhsiungchelyidae) from the Upper Cretaceous of Nanxiong Basin, China

Yuzheng Ke<sup>Corresp., 1</sup>, Imran A Rahman<sup>2,3</sup>, Hanchen Song<sup>1</sup>, Jinfeng Hu<sup>1</sup>, Kecheng Niu<sup>4</sup>, Fasheng Lou<sup>5</sup>, Hongwei Li<sup>6</sup>, Fenglu Han<sup>Corresp., 1</sup>

<sup>1</sup> School of Earth Science, China University of Geosciences (Wuhan), Wuhan, Hubei, People's Republic of China

<sup>2</sup> The Natural History Museum, London, United Kingdom

<sup>3</sup> Oxford University Museum of Natural History, Oxford, United Kingdom

<sup>4</sup> Yingliang Stone Natural History Museum, Nan'an, Fujian, People's Republic of China

<sup>5</sup> Jiangxi Geological Survey and Exploration Institute, Nanchang, Jiangxi, People's Republic of China

<sup>6</sup> Guangdong Geological Survey Institute, Guangzhou, Guangdong, People's Republic of China

Corresponding Authors: Yuzheng Ke, Fenglu Han  
Email address: key1480@163.com, hanfl@cug.edu.cn

Nanhsiungchelyidae are a group of large turtles that lived in Asia and North America during the Cretaceous. Here we report a new species of nanhsiungchelyid, *Nanhsiungchelys yangi* sp. nov., from the Upper Cretaceous of Nanxiong Basin, China. The specimen consists of a well-preserved skull and lower jaw, as well as the anterior parts of the carapace and plastron. The diagnostic features of *Nanhsiungchelys* include a huge entire carapace length (~55.5 cm), a network of sculptures consisting of pits and ridges on the surface of the skull and shell, shallow cheek emargination and temporal emargination, deep nuchal emargination, and a pair of anterolateral processes on the carapace. However, *Nanhsiungchelys yangi* differs from the other species of *Nanhsiungchelys* mainly in having a triangular-shaped snout (in dorsal view) and wide anterolateral processes. Besides, some other characteristics (e.g. the premaxilla is higher than wide, the maxilla is unseen in dorsal views, a small portion of the maxilla extends posterior and ventral of the orbit, and the parietal is bigger than the frontal) are strong evidences to distinguish *Nanhsiungchelys yangi* from *Nanhsiungchelys wuchinensis*. A phylogenetic analysis of nanhsiungchelyids places *Nanhsiungchelys yangi* and *Nanhsiungchelys wuchingensis* as sister taxa. *Nanhsiungchelys yangi* and some other nanhsiungchelyids bear distinct anterolateral processes on the carapace, which have not been reported in any extant turtles and may have played a role in protecting the head. Nanxiong Basin was extremely hot during the Late Cretaceous, and so we suggest that nanhsiungchelyids might have immersed themselves in mud or water to avoid the hot weather, similar to some extant tortoises. If they were capable of swimming, our computer simulations of fluid flow suggest

the anterolateral processes could have reduced drag during locomotion.

1  
2 **A new species of *Nanhsiungchelys* (Testudines:**  
3 **Cryptodira: Nanhsiungchelyidae) from the Upper**  
4 **Cretaceous of Nanxiong Basin, China**

5  
6  
7 Yuzheng Ke<sup>1</sup>, Imran A. Rahman<sup>2,3</sup>, Hanchen Song<sup>1</sup>, Jinfeng Hu<sup>1</sup>, Kecheng Niu<sup>4</sup>, Fasheng Lou<sup>5</sup>,  
8 Hongwei Li<sup>6</sup>, Fenglu Han<sup>1</sup>

9 <sup>1</sup> School of Earth Science, China University of Geosciences (Wuhan), Wuhan, Hubei, China.

10 <sup>2</sup> The Natural History Museum, London, UK.

11 <sup>3</sup> Oxford University Museum of Natural History, Oxford, UK.

12 <sup>4</sup> Yingliang Stone Natural History Museum, Nan'an, Fujian, China

13 <sup>5</sup> Jiangxi Geological Survey and Exploration Institute, Nanchang, Jiangxi, China

14 <sup>6</sup> Guangdong Geological Survey Institute, Guangzhou, Guangdong, China

15  
16 Corresponding Author:

17 Fenglu Han

18 Lumo Road, Wuhan, Hubei, 430074, China

19 Email address: hanfl@cug.edu.cn

20 Yuzheng Ke

21 Lumo Road, Wuhan, Hubei, 430074, China

22 Email address: key1480@163.com

23  
24 **Abstract**

25 Nanhsiungchelyidae are a group of large turtles that lived in Asia and North America during the  
26 Cretaceous. Here we report a new species of nanhsiungchelyid, *Nanhsiungchelys yangi* sp. nov.,  
27 from the Upper Cretaceous of Nanxiong Basin, China. The specimen consists of a well-  
28 preserved skull and lower jaw, as well as the anterior parts of the carapace and plastron. The  
29 diagnostic features of *Nanhsiungchelys* include a huge entire carapace length (~55.5 cm), a  
30 network of sculptures consisting of pits and ridges on the surface of the skull and shell, shallow  
31 cheek emargination and temporal emargination, deep nuchal emargination, and a pair of  
32 anterolateral processes on the carapace. However, *Nanhsiungchelys yangi* differs from the other  
33 species of *Nanhsiungchelys* mainly in having a triangular-shaped snout (in dorsal view) and wide  
34 anterolateral processes. Besides, some other characteristics (e.g. the premaxilla is higher than  
35 wide, the maxilla is unseen in dorsal views, a small portion of the maxilla extends posterior and  
36 ventral of the orbit, and the parietal is bigger than the frontal) are strong evidences to distinguish  
37 *Nanhsiungchelys yangi* from *Nanhsiungchelys wuchinensis*. A phylogenetic analysis of  
38 nanhsiungchelyids places *Nanhsiungchelys yangi* and *Nanhsiungchelys wuchingensis* as sister

39 taxa. *Nanhsiungchelys yangi* and some other nanhsiungchelyids bear distinct anterolateral  
40 processes on the carapace, which have not been reported in any extant turtles and may have  
41 played a role in protecting the head. Nanxiong Basin was extremely hot during the Late  
42 Cretaceous, and so we suggest that nanhsiungchelyids might have immersed themselves in mud  
43 or water to avoid the hot weather, similar to some extant tortoises. If they were capable of  
44 swimming, our computer simulations of fluid flow suggest the anterolateral processes could have  
45 reduced drag during locomotion.

46

## 47 Introduction

48 Nanhsiungchelyidae are an extinct group of Pan-Trionychia, which lived in Asia and North  
49 America from the Early Cretaceous until their extinction at the Cretaceous–Paleogene boundary  
50 (*Hirayama et al., 2000; Li & Tong, 2017; Joyce et al., 2021*). These turtles are characterized by a  
51 large body size (maximum entire carapace length of 111 cm) (*Tong & Li, 2019*), flat carapace  
52 relative to tortoises (*Brinkman et al., 2015*), stubby elephantine limbs (*Yeh, 1966; Hutchison &*  
53 *Archibald, 1986*), and shells covered with a network of sculptures consisting of pits and ridges  
54 (*Li & Tong, 2017*). In addition, these turtles produced thick-shelled (~1.8 mm) eggs and are  
55 thought to have had similar reproductive strategies to extant tortoises (e.g. large and spherical  
56 eggs) (*Ke et al., 2021*). Recently, the morphology and phylogenetic relationships of  
57 nanhsiungchelyids have been studied in detail (*Danilov et al., 2013; Brinkman et al., 2015; Tong*  
58 *et al., 2016; Mallon & Brinkman, 2018; Tong & Li, 2019*). Among the eight genera of  
59 Nanhsiungchelyidae, most taxa typically have a relatively short carapace, shallow nuchal  
60 emargination, narrow neurals and vertebral scutes, and lack large anterior processes on the  
61 carapace (*Tong & Li, 2019*). In contrast, *Nanhsiungchelys* and *Anomalochelys* (which form a  
62 sister group) share an elongated shell, huge nuchal emargination, large anterior process on the  
63 carapace, wide neurals and vertebral scutes, and a sub-triangular first vertebral scute with a very  
64 narrow anterior end (*Tong & Li, 2019*). These two genera have only been found in southern  
65 China and Japan (*Hirayama et al., 2001; Hirayama et al., 2009; Li & Tong, 2017; Tong & Li,*  
66 *2019*), whereas other nanhsiungchelyids have a wider geographical distribution (*Danilov &*  
67 *Syromyatnikova, 2008; Mallon & Brinkman, 2018*).

68 *Nanhsiungchelys* and *Anomalochelys* are unique among Mesozoic turtles in possessing distinct  
69 anterolateral processes on the carapace, with a similar body structure known in the Miocene side-  
70 necked turtle *Stupendemys geographicus* (*Cadena et al., 2020*). Palaeontologists have debated  
71 whether nanhsiungchelyids were aquatic or terrestrial for nearly 60 years (see *Mallon &*  
72 *Brinkman (2018)* for a detailed overview), but the ecological role of the anterolateral processes  
73 has largely been ignored. It was previously suggested they played a role in protecting the head  
74 (*Hirayama et al., 2001*), but further study of their function is required.

75 In China, five species of nanhsiungchelyids have been reported (Table 1), with many  
76 specimens recovered from the Upper Cretaceous of Nanxiong Basin, Guangdong Province. *Yeh*  
77 (*1966*) described the first species, *Nanhsiungchelys wuchingensis*, which was restudied by *Tong*  
78 *& Li (2019)*. *Hirayama et al., (2009)* provided a preliminary study of a large Cretaceous turtle

79 (SNHM 1558) which they placed within Nanhsiungchelyidae; *Li & Tong (2017)* later attributed  
80 this to *Nanhsiungchelys*. In addition, two eggs (IVPP V2789) from Nanxiong Basin were  
81 assigned to nanhsiungchelyids based on their co-occurrence with *Nanhsiungchelys wuchingensis*  
82 (*Young, 1965*).

83 Nanxiong Basin (Fig. 1A) is a NE-trending faulted basin controlled by the Nanxiong Fault in  
84 the northern margin, covering an area of about 1800 km<sup>2</sup> and spanning Guangdong and Jiangxi  
85 provinces in China (*Zhang et al., 2013*). There are well-exposed outcrops of Cretaceous–  
86 Paleogene strata in Nanxiong Basin (*Ling et al., 2005*), and the lithostratigraphy of the Upper  
87 Cretaceous in this region has been studied extensively (see *Zhang et al. (2013)* for details). In  
88 1966, the holotype of *Nanhsiungchelys wuchingensis* (IVPP V3106) was recovered from  
89 Nanxiong Basin, with the stratum where the fossil was found named the Nanxiong Group (*Yeh*  
90 *1966*). Subsequently, *Zhao et al. (1991)* split Nanxiong Group into the upper Pingling Formation  
91 and lower Yuanpu Formation, reporting two K–Ar ages for the Yuanpu Formation (67.04±2.31  
92 Ma and 67.37±1.49 Ma). *Zhang et al. (2013)* further divided the original Yuanpu Formation into  
93 the Jiangtou, Yuanpu, Dafeng, and Zhutian formations, with the new Yuanpu Formation just a  
94 small part of the original Yuanpu Formation. Most recently, the Yuanpu Formation was  
95 eliminated entirely and the Nanxiong Group now consists of Dafeng, Zhutian, and Zhenshui  
96 formations (*Guangdong Geological Survey Institute, 2017*). This terminology was also used by  
97 *Xi et al. (2021)*, who summarized lithostratigraphic subdivision and correlation for the  
98 Cretaceous of China. Under this scheme, the holotype of *Nanhsiungchelys wuchingensis* (IVPP  
99 V3106) and *N. yangi* (CUGW VH108, see below) both come from the Dafeng Formation.

100 The Dafeng Formation comprises purple-red, brick-red, and brownish-red conglomerate,  
101 sandy conglomerate, and gravel-bearing sandstone, and is intercalated with sandstone, siltstone  
102 and silty mudstone (*Guangdong Geological Survey Institute, 2017*). It ranges in age from the  
103 Cenomanian to the middle Campanian (*Xi et al., 2021*). In addition to *Nanhsiungchelys*, many  
104 vertebrate fossils have been recovered from the Dafeng Formation, including: the dinosaur  
105 *Nanshiungosaurus brevispinus* (*Zanno, 2010*); the turtle eggs *Oolithes nanhsiungensis* (*Young,*  
106 *1965*); and the dinosaur eggs *Macroolithus rugustus*, *Nanhsiungoolithus chuetienensis*,  
107 *Ovaloolithus shitangensis*, *O. nanxiongensis*, and *Shixingoolithus erbeni* (*Zhao et al., 2015*).

108 Here, we report a new species of *Nanhsiungchelys* from Nanxiong Basin based on a complete  
109 skull and partial postcranial skeleton. This allows us to investigate the taxonomy and  
110 morphology of nanhsiungchelyids, and based on this we carry out a phylogenetic analysis of the  
111 group. In addition, we discuss potential functions of the large anterolateral processes (using  
112 computational fluid dynamics to test a possible role in drag reduction) and consider the  
113 implications for the ecology of this taxon.

114

## 115 **Materials & Methods**

116 **Fossil specimen.** The specimen (CUGW VH108) consists of a well-preserved skull and lower  
117 jaw, together with the anterior parts of the carapace and plastron (Figs. 2–4). This  
118 specimen was found in southeast of Nanxiong Basin, near the Zhenjiang River. Based on the

119 brownish-red siltstone near the skeleton, it was definitely from the Dafeng Formation  
120 (*Guangdong Geological Survey Institute, 2017*). CUGW VH108 is housed in the paleontological  
121 collections of China University of Geosciences (Wuhan). The skeleton was prepared using an  
122 Engraving Pen AT-310, and was photographed with a Canon EOS 6D camera.

123 **Nomenclatural acts.** The electronic version of this article in Portable Document Format (PDF)  
124 will represent a published work according to the International Commission on Zoological  
125 Nomenclature (ICZN), and hence the new names contained in the electronic version are  
126 effectively published under that Code from the electronic edition alone. This published work and  
127 the nomenclatural acts it contains have been registered in ZooBank, the online registration  
128 system for the ICZN. The ZooBank LSIDs (Life Science Identifiers) can be resolved and the  
129 associated information viewed through any standard web browser by appending the LSID to the  
130 prefix <http://zoobank.org/>. The LSID for this publication is:  
131 [urn:lsid:zoobank.org:pub:F53B5FA5-D018-453D-814D-C854810EFEFE](http://zoobank.org/pub:F53B5FA5-D018-453D-814D-C854810EFEFE). The online version of  
132 this work is archived and available from the following digital repositories: PeerJ, PubMed  
133 Central SCIE and CLOCKSS.

134 **Phylogenetic analysis.** Parsimony phylogenetic analysis was performed using the software TNT  
135 1.5 (*Goloboff & Catalano, 2016*). The data matrix used herein was updated from *Tong & Li,*  
136 *(2019)* and *Mallon & Brinkman, (2018)*, and includes 17 taxa and 50 characters. Because there  
137 are five inframarginal scutes on *Jiangxichelys ganzhouensis* (*Tong et al., 2016*), character 37 was  
138 modified to: “Inframarginals: (0) five to three pairs; (1) two pairs; (2) absent”. In addition,  
139 character 48 was changed in *Jiangxichelys ganzhouensis* from ? to 1 (i.e. ratio of midline  
140 epiplastral suture length to total midline plastral length greater than 0.1). The length to width  
141 ratios of the carapace of *Nanhsiungchelys* and *Anomalochelys* are equal to or larger than 1.6  
142 (*Hirayama et al., 2001; Hirayama et al., 2009; Tong & Li, 2019*), whereas the other genera (e.g.  
143 *Basilemys*) exhibit smaller ratios (*Mallon & Brinkman, 2018*). The ratio that between 1.4 and 1.6  
144 has not been found in any nanhsiungchelyids yet. Therefore, a new character was added: “Length  
145 to width ratio of the carapace: (0) less than 1.4; (1) equal to or larger than 1.6”. Moreover,  
146 *Yuchelys nanyangensis* was added to the data matrix based on *Tong et al., (2012)*. A total of 13  
147 characters out of 50 could be coded for *Nanhsiungchelys yangi*, representing only 26% of the  
148 total number of characters. This is because the new species is based on a partial specimen  
149 missing many of the features scored in other taxa. The analysis was conducted using a traditional  
150 search with 1000 replicates. A tree bisection reconnection (TBR) swapping algorithm was  
151 employed, and 10 trees were saved per replicate. All characters were treated as unordered and of  
152 equal weight. Standard bootstrap support values were calculated using a traditional search with  
153 100 replicates. Bremer support values were also calculated (*Bremer, 1994*). In addition, a time-  
154 scaled phylogeny was generated in R (<https://www.r-project.org/>) using our strict consensus tree  
155 and the first / last appearance datum (FAD / LAD) of all taxa. The R package Strap (*Bell &*  
156 *Lloyd, 2014*) was used to estimate divergence times and the function *geoscalePhylo* was used to  
157 plot the time-scaled tree against a geological timescale.

158 **Computational fluid dynamics.** Computational fluid dynamics (CFD) simulations of water  
159 flow were performed in the software COMSOL Multiphysics (v. 5.6). Three-dimensional digital  
160 models of *Nanhsiungchelys yangi* and two ‘hypothetical turtles’ without anterolateral processes  
161 were created using COMSOL’s in-built geometry tools. These models were placed in cylindrical  
162 flow domains, with the material properties of water assigned to the space surrounding the models  
163 and the swimming speeds of the extant large turtle used as flow velocities at the inlet. CFD  
164 simulations were performed using a stationary solver, and based on the results drag forces were  
165 extracted for each model. The main steps including the construction of digital models,  
166 specification of fluid properties and boundary conditions, meshing, and computation are detailed  
167 in Supplemental Information 3.

168 **Institutional abbreviations.** CUGW, China University of Geosciences (Wuhan), Wuhan, China;  
169 HGM, Henan Geological Museum, Zhengzhou, China; IMM, Inner Mongolia Museum, Huhhot,  
170 China; IVPP, Institute of Vertebrate Paleontology and Paleoanthropology, Chinese Academy of  
171 Sciences, Beijing, China; LJU, Lanzhou Jiaotong University, Lanzhou, China; NHMG, Natural  
172 History Museum of Guangxi, Nanning, China; NMBY, Nei Mongo Bowuguan, Huhhot, China;  
173 SNHM, Shanghai Natural History Museum, Shanghai, China; UB, University of Bristol, Bristol,  
174 UK; UPC, China University of Petroleum (East China), Qingdao, China; YSNHM, Yingliang  
175 Stone Nature History Museum, Nan’an, China.

176

## 177 **Results**

### 178 **Systematic paleontology**

179 Order Testudines Linnaeus, 1758

180 Infraorder Cryptodira Cope, 1868

181 Family Nanhsiungchelyidae Yeh, 1966

182 Genus *Nanhsiungchelys* Yeh, 1966

183 **Emended diagnosis.** A genus of Nanhsiungchelyidae of medium-large size, with an entire  
184 carapace length of 0.5–1.1 m. The surface of the skull, lower jaw, and both carapace and plastron  
185 are covered with sculptures consisting of large pits formed by a network of ridges. Temporal  
186 emargination and cheek emargination are shallow; orbits located at about mid-length of the skull  
187 and facing laterally; jugal forms the lower margin of the orbit. Carapace elongate, with a deep  
188 nuchal emargination and a pair of large anterolateral processes that extend forward and are  
189 formed entirely by the first peripheral; wide neural plates and vertebral scutes; gulars fused and  
190 extend deeply onto the entoplastron; extragulars absent; complete row of narrow inframarginals.  
191 Wide angle between the acromion process and scapula process of about 105°. One large dermal  
192 plate located above the manus.

193 **Type species.** *Nanhsiungchelys wuchingensis* Yeh, 1966

194 **Distribution.** Guangdong, China

195

196 Species *Nanhsiungchelys yangi* sp. nov.

197 **Etymology.** *Yangi* is in memory of paleontologist Zhongjian Yang (Chung-Chien Young).

198 **Holotype.** CUGW VH108, a partial skeleton comprising a well-preserved skull and lower jaw  
199 and the anterior parts of the carapace and plastron (Figs. 2–4).

200 **Locality and horizon.** Nanxiong, Guangdong, China. Dafeng Formation, Upper Cretaceous,  
201 Cenomanian to middle Campanian (*Xi et al., 2021*).

202 **Diagnosis.** A medium-sized species of *Nanhsiungchelys* with an estimated entire carapace length  
203 of more than 0.5 meters. It differs from other species of *Nanhsiungchelys* in the following  
204 combination of characters: the snout is triangular in dorsal view; the premaxilla greater in height  
205 than length; the posteroventral ramus of the maxilla extends to the ventral region of the orbit; the  
206 dorsal margin of the maxilla is relatively straight; the jugal is greater in height than width; the  
207 prefrontal is convex dorsally behind the naris; the temporal emargination is mainly formed by the  
208 parietal; the paired parietals are bigger than the frontals in dorsal view; the middle and posterior  
209 parts of the mandible are more robust than the most anterior part in ventral view; the  
210 anterolateral processes is wide; and the angle between the two anterior edges of the entoplastron  
211 is wide ( $\sim 110^\circ$ ).

212 **Description.**

213 **General aspects of the skull.** The skull is large, with a length of 13 cm (Fig. 3A, B). It is well  
214 preserved but there are many cracks on its outer surface, which limit the identification of bone  
215 sutures. The snout (i.e. the parts anterior to the orbit) is large, equal to about 1/3 length of the  
216 skull, and longer than in *Jiangxichelys neimongolensis* and *Zangerlia ukhaachelys* (*Joyce &*  
217 *Norell, 2005; Brinkman et al., 2015*). In dorsal view, the snout is close to triangular in outline  
218 with a narrow anterior end (Fig. 3A, B). In lateral views, the robust snout is nearly as deep as the  
219 whole skull, with the anterior end roughly perpendicular to the horizon (Fig. 3C–F). These  
220 features differ from *Nanhsiungchelys wuchingensis* in which the snout is flattened, with the  
221 anterior end increasing in width in dorsal view (*Tong & Li, 2019*), giving it a trumpet shape. A  
222 large naris is located in the front part of the snout, which is roughly lozenge shaped and greater  
223 in height than width in anterior view (Fig. 2). Because the posterior part of the skull is not  
224 preserved, it is difficult to accurately determine the morphological characteristics of cheek  
225 emargination (Fig. 3C–F). Nevertheless, based on the visible bone morphology, we infer that the  
226 cheek emargination was absent or low, rather than deep (i.e. to the level or even beyond the level  
227 of orbit, see e.g. *Emydura macquarrii*) (*Li & Tong, 2017*). Posteriorly, the temporal emargination  
228 is weakly developed (Fig. 3A, B), which is similar to *Nanhsiungchelys wuchingensis* (*Tong & Li,*  
229 *2019*), but differs from *Jiangxichelys neimongolensis*, *J. ganzhouensis* and *Zangerlia*  
230 *ukhaachelys* (*Brinkman & Peng, 1996; Joyce & Norell, 2005; Tong et al., 2016*). The surface of  
231 the skull (and the carapace and plastron) is covered with a network of sculptures consisting of  
232 pits and ridges, which is a synapomorphy of Nanhsiungchelyidae (*Li & Tong, 2017*).

233 **Premaxilla.** A small bone in the anterior and ventral part of the maxilla is identified as the  
234 premaxilla (Fig. 3C–F). It is greater in height than width, similar to *Jiangxichelys*  
235 *neimongolensis* and *Zangerlia ukhaachelys* (*Joyce & Norell, 2005; Brinkman et al., 2015*), but  
236 differs from *Nanhsiungchelys wuchingensis* in which the premaxilla is wider than it is high in  
237 lateral view and has an inverse Y-shape in ventral view (*Tong & Li, 2019*). Given the existence

238 of the large lozenge-shaped external narial opening, the left and right premaxillae may not have  
239 been in contact each other, unlike the condition of *Jiangxichelys neimongolensis* and *Zangerlia*  
240 *ukhaachelys* (Joyce & Norell, 2005; Brinkman et al., 2015). However, the poor preservation of  
241 elements near the external narial opening prevents more detailed observations, and the possibility  
242 of a Y-shaped premaxilla as in *Nanhsiungchelys wuchingensis* cannot be excluded.

243 **Maxilla.** The maxilla is large and trapezoid in outline (Fig. 3C–F). The main body is located  
244 anterior to the orbit, but the posteroventral ramus extends to the ventral region of the orbit, which  
245 differs from the situation in *Nanhsiungchelys wuchingensis* in which the maxilla is located  
246 entirely anterior to the orbit (Tong & Li, 2019), and also differs from most other turtles  
247 (including *Zangerlia ukhaachelys* and *Jiangxichelys neimongolensis*) in which the maxilla  
248 contributes to the lower rim of the orbit (Joyce & Norell, 2005; Brinkman et al., 2015). In lateral  
249 view, the dorsal margin of the maxilla is relatively straight and extends posteriorly to the mid-  
250 region of the eye socket, which is similar to some extant turtles (e.g. *Platysternon*  
251 *megacephalum*) (Li & Tong, 2017). However, this differs from *Nanhsiungchelys wuchingensis* in  
252 which the top of the maxilla is curved dorsally (Tong & Li, 2019), and also differs from  
253 *Zangerlia ukhaachelys* and *Jiangxichelys neimongolensis* in which the top of the maxilla tapers  
254 anterodorsally (Joyce & Norell, 2005; Brinkman et al., 2015).

255 **Jugal.** The jugal is shaped like a parallelogram in lateral view (Fig. 3C–F). It is greater in height  
256 than width, unlike *Nanhsiungchelys wuchingensis* in which the jugal is wider than it is high  
257 (Tong & Li, 2019). The jugal consists of the lower rim of the orbit, which is similar to  
258 *Nanhsiungchelys wuchingensis*, but differs from most turtles in which this structure is mainly  
259 formed by the maxilla (Tong & Li, 2019). The jugal of *Nanhsiungchelys yangi* also differs from  
260 that of *Jiangxichelys ganzhouensis* in which the jugal is more posteriorly located (Tong et al.,  
261 2016). The jugal contacts with the maxilla anteriorly, and this suture is sloped. The terminal parts  
262 of the jugal contacts with the quadratojugal.

263 **Quadratojugal.** The bone that is posterior to the jugal and ventral to the postorbital is identified  
264 as the quadratojugal (Fig. 3C–F). Its location is similar in *Nanhsiungchelys wuchingensis* (Tong  
265 & Li, 2019), but the full shape is uncertain due to covering by the carapace.

266 **Prefrontal.** In dorsal view, each prefrontal is large and elongate anteroposteriorly, and narrows  
267 anteriorly and enlarges posteriorly (Fig. 3A, B). The portion in front of the orbit is entirely  
268 composed of the prefrontal (Fig. 3A, B), which differs from *Nanhsiungchelys wuchingensis* in  
269 which the maxilla extends dorsally to the prefrontal and occupies some space (Tong & Li, 2019).  
270 The paired prefrontals contact each other at the midline and form an approximate arrow shape.  
271 They form the dorsal margin of naris anteriorly, the anterodorsal rim of the orbit posterolaterally,  
272 and contact the frontal and postorbital posteriorly (Fig. 3A, B). The contact area between the  
273 prefrontal and frontal is convex anteriorly (i.e. ‘Λ’-shaped), which is similar to *Nanhsiungchelys*  
274 *wuchingensis* (Tong & Li, 2019). In lateral view, the prefrontal is anterior to the postorbital and  
275 dorsal to the maxilla, and consists of the anterodorsal rims of the orbit (Fig. 3C–F). This is  
276 similar to *Nanhsiungchelys wuchingensis*, *Jiangxichelys neimongolensis* and *Zangerlia*  
277 *ukhaachelys* (Brinkman & Peng, 1996; Joyce & Norell, 2005; Tong & Li, 2019). Behind the

278 naris, the prefrontal is convex dorsally (Fig. 3C–F), rather than concave as in *Nanhsiungchelys*  
279 *wuchingensis* (Tong & Li, 2019).

280 **Frontal.** The paired frontals form a large pentagon that locate in the center of the skull roof (Fig.  
281 3A, B), which is similar to *Nanhsiungchelys wuchingensis* and *Zangerlia ukhaachelys* (Joyce &  
282 Norell, 2005; Tong & Li, 2019). Their anterior margins constitute of a “Λ” shape for articulating  
283 with the prefrontal. The lateral and posterior margins contact the postorbital and parietal  
284 respectively. The frontal is excluded from the rim of the orbit, as in *Nanhsiungchelys*  
285 *wuchingensis* and *Zangerlia ukhaachelys* (Joyce & Norell, 2005; Tong & Li, 2019). Notably,  
286 there is a line between the paired of frontals (Fig. 3A, B), which might be a suture or crack. We  
287 think it most likely represents a suture since a similar structure appears in other nanhsiungchelyid  
288 specimens (Joyce & Norell, 2005; Tong & Li, 2019). Interestingly, this suture is unusually  
289 slanted, which may be the result of developmental abnormality and needs more specimens for  
290 verification.

291 **Postorbital.** The postorbital is subtriangular in outline and elongated anteroposteriorly, and it  
292 consists of part of the lateral skull roof. Most parts of the postorbital are behind the orbit, but the  
293 anterodorsal process extends to the dorsal edge of the orbit (Fig. 3C–F). Thus, the postorbital  
294 consists of the posterior-upper and posterior rims of the orbits, which is similar to  
295 *Nanhsiungchelys wuchingensis*, *Jiangxichelys ganzhouensis* and *Zangerlia ukhaachelys* (Joyce  
296 & Norell, 2005; Tong et al., 2016; Tong & Li, 2019). The postorbital contacts the prefrontal and  
297 frontal anteriorly, the jugal and quadratojugal ventrally, and the parietal medially (Fig. 3A–F). In  
298 dorsal view, the shape of the posterior margin of the postorbital is uncertain due to its poor  
299 preservation and because it is partly obscured by the carapace. It is also uncertain if the  
300 postorbital constitutes the rim of temporal emargination. Notably, the postorbital in both  
301 *Nanhsiungchelys yangi* and *N. wuchingensis* is relatively large in size (Tong & Li, 2019),  
302 whereas just a small element forms the ‘postorbital bar’ in *Jiangxichelys ganzhouensis* and  
303 *Zangerlia ukhaachelys* (Joyce & Norell, 2005; Tong et al., 2016).

304 **Parietal.** The trapezoidal parietal contributes to the posterior part of the skull roof (Fig. 3A, B),  
305 which is similar to *Nanhsiungchelys wuchingensis* (Tong & Li, 2019). However, the paired  
306 parietals are bigger than the frontals in dorsal view, contrasting with *Nanhsiungchelys*  
307 *wuchingensis* (Tong & Li, 2019). The parietal contacts the frontal anteriorly and the postorbital  
308 laterally, and these boundaries are not straight. Posteriorly, the parietal contributes to the upper  
309 temporal emarginations, but the absence of the posterior ends of the parietal (especially the right  
310 part) hampers the identification of the rim of upper temporal emarginations.

311 **Mandible.** The mandible is preserved in situ and tightly closed with the skull (Fig. 3C–F). The  
312 location of the mandible is posterior and interior to the maxillae (Fig. 4). As a result, the beak is  
313 hidden, but the lower parts of the mandible can be observed. The symphysis is fused, which is  
314 similar to *Nanhsiungchelys wuchingensis* (Tong & Li, 2019). In ventral view, the most anterior  
315 part of the mandible appears slender, but the middle and posterior parts are robust (Fig. 4). This  
316 differs from *Nanhsiungchelys wuchingensis* in which nearly all parts of the mandible are equal in  
317 width (Tong & Li, 2019).

318 **Carapace.** Only the anterior parts of the carapace are preserved (Fig. 3A, B). The preserved  
319 parts indicate there is a deep nuchal emargination and a pair of anterolateral processes, which are  
320 similar to those of *Anomalochelys angulata*, *Nanhsiungchelys wuchingensis* and *N. sp.* (SNHM  
321 1558) (Hirayama et al., 2001; Hirayama et al., 2009; Tong & Li, 2019). In contrast, the  
322 carapaces of other genera of nanhsiungchelyids (including *Basilemys*, *Hanbogdemys*,  
323 *Kharakhutulia*, *Jiangxichelys* and *Zangerlia*) usually have a shallow nuchal emargination and/or  
324 lack the distinctive anterolateral processes (Mlynarski, 1972; Sukhanov, 2000; Sukhanov et al.,  
325 2008; Tong & Mo, 2010; Danilov et al., 2013; Mallon & Brinkman, 2018). In dorsal view, each  
326 anterolateral process of *Nanhsiungchelys yangi* is very wide (nearly 90°), similar to  
327 *Nanhsiungchelys wuchingensis* (Tong & Li, 2019); however, the anterolateral processes of  
328 *Anomalochelys angulata* and *Nanhsiungchelys sp.* (SNHM 1558) are slender crescent-shaped  
329 and horn-shaped, respectively, both of which are sharper than in *Nanhsiungchelys yangi*  
330 (Hirayama et al., 2001; Hirayama et al., 2009). Among the above species of *Nanhsiungchelys*  
331 and *Anomalochelys*, there is always a distinct protrusion at the tip of each anterolateral process,  
332 and this protrusion becomes more prominent in *Anomalochelys angulata* (Fig. 5B) and  
333 *Nanhsiungchelys sp.* (SNHM 1558) (Hirayama et al., 2001; Hirayama et al., 2009). In  
334 *Nanhsiungchelys wuchingensis* and *Anomalochelys angulata* the most anterior end of the process  
335 shows varying degrees of bifurcation (Fig. 5B) (Hirayama et al., 2001; Tong & Li, 2019), but  
336 this bifurcation does not occur in *Nanhsiungchelys yangi* and *N. sp.* (SNHM 1558) (Hirayama et  
337 al., 2009). Due to the lack of sutures preserved on the surface of the carapace, it is difficult to  
338 determine whether these processes are composed of nuchal or peripheral plates. However,  
339 considering the similarity in shape of the anterolateral processes in *Nanhsiungchelys yangi* and  
340 *N. wuchingensis*, the anterolateral processes of *N. yangi* may be formed by the first peripheral  
341 plates (as in *N. wuchingensis*).

342 **Plastron.** A large plate under the mandible is identified as the anterior part of the plastron (Fig.  
343 4). The anterior edge of the epiplastron extends anteriorly beyond the deepest part of nuchal  
344 emargination (Fig. 4), similar to *Basilemys*, *Hanbogdemys*, *Jiangxichelys*, *Nanhsiungchelys*, and  
345 *Zangerlia* (Sukhanov, 2000; Danilov et al., 2013; Brinkman et al., 2015; Tong et al., 2016;  
346 Mallon & Brinkman, 2018; Tong & Li, 2019). The anterior part of the epiplastron is very thin,  
347 but it increases in thickness posteriorly and laterally (Fig. 2). Although poorly preserved, the  
348 angle between the left and right edges can be measured as about 55°, which is wider than  
349 *Hanbogdemys orientalis* (Sukhanov, 2000). The epiplastra are paired and connected at the  
350 midline. Because only the anterior part of the entoplastron is preserved, it is hard to recognize its  
351 shape. The anterior edges of the entoplastron are strongly convex, and lead into the posterior part  
352 of the epiplastra. The angle between the two anterior edges (>110°) is larger than in  
353 *Nanhsiungchelys wuchingensis* (~100°) (Tong & Li, 2019). The only identifiable scutes are the  
354 gular and the humeral. In many nanhsiungchelyids, like *Basilemys praeclara*, *Basilemys*  
355 *morrinensis*, *Jiangxichelys ganzhouensis*, *J. neimongolensis*, *Hanbogdemys orientalis*, *Zangerlia*  
356 *dzamynchondi* and *Kharakhutulia kalandadzei* (Brinkman & Nicholls, 1993; Brinkman & Peng,  
357 1996; Sukhanov, 2000; Sukhanov et al., 2008; Danilov et al., 2013; Tong et al., 2016; Mallon &

358 *Brinkman, 2018*), there are usually extragular scutes beside the gular scutes, but this does not  
359 occur in *Nanhsiungchelys wuchingensis* (*Tong & Li, 2019*) and *N. yangi*. Moreover, the location  
360 and shape of the sulci of *Nanhsiungchelys yangi* are similar to *N. wuchingensis* (*Tong & Li,*  
361 *2019*). In *Nanhsiungchelys yangi*, the sulcus between the gular and humeral scutes can be  
362 identified and it is slightly curved and extend onto the entoplastron, which is similar to  
363 *Jiangxichelys neimongolensis* and *Nanhsiungchelys wuchingensis* (*Brinkman & Peng, 1996;*  
364 *Brinkman et al., 2015; Tong & Li, 2019*). However, in the other nanhsiungchelyids (e.g.  
365 *Kharakhutulia kalandadzei, Zangerlia dzamynchondi, Hanbogdemys orientalis, Yuchelys*  
366 *nanyangensis* and *Jiangxichelys ganzhouensis*), this sulcus is tangential to (or separated from)  
367 the entoplastron (*Sukhanov, 2000; Sukhanov et al., 2008; Tong et al., 2012; Danilov et al., 2013;*  
368 *Tong et al., 2016*).

369

## 370 Discussion

### 371 Taxonomy

372 Through comparison with a complete specimen (IVPP V3106) of *Nanhsiungchelys*  
373 *wuchingensis*, the large skull (length = 13 cm) of CUGW VH108 is inferred to correspond to an  
374 entire carapace length of ~55.5 cm (Please see Fig. 5A for a definition of ‘entire carapace  
375 length’, which comes from *Hirayama et al. (2001)*). This large body size, coupled with the  
376 network of sculptures on the surface of the skull and shell, clearly demonstrates that CUGW  
377 VH108 belongs to Nanhsiungchelyidae (*Li & Tong, 2017*). Moreover, CUGW VH108 has a  
378 laterally thickened epiplastron (Fig. 2), with the anterior edge of the epiplastron extending  
379 anterior of the deepest part of nuchal emargination (Fig. 4), additional features that are diagnostic  
380 of Nanhsiungchelyidae (*Li & Tong, 2017*).

381 Within Nanhsiungchelyidae, CUGW VH108 differs from *Basilemys, Hanbogdemys,*  
382 *Kharakhutulia, Yuchelys,* and *Zangerlia* because all of these taxa have weak nuchal emargination  
383 and/or lack distinct anterolateral processes (*Mlynarski, 1972; Sukhanov, 2000; Sukhanov et al.,*  
384 *2008; Tong et al., 2012; Danilov et al., 2013; Mallon & Brinkman, 2018*). Moreover, CUGW  
385 VH108 differs from *Jiangxichelys ganzhouensis* and *J. neimongolensis* in which the cheek  
386 emargination and temporal emargination are deep (*Brinkman & Peng, 1996; Tong et al., 2016*).  
387 Although the carapace of both *Anomalochelys* and CUGW VH108 have deep nuchal  
388 emargination and a pair of anterolateral processes, the former’s anterolateral processes are  
389 slender crescent-shaped and have a bifurcated anterior end (*Hirayama et al., 2001*), which are  
390 clear differences from the wide processes of CUGW VH108.

391 CUGW VH108 is assigned to the genus *Nanhsiungchelys* based on the deep nuchal  
392 emargination, pair of anterolateral processes, and weakly developed cheek emargination and  
393 temporal emargination (*Li & Tong, 2017*). However, CUGW VH108 differs from  
394 *Nanhsiungchelys wuchingensis* in which the snout is trumpet shaped (*Tong & Li, 2019*).  
395 Moreover, *Nanhsiungchelys wuchingensis* and CUGW VH108 show some differences in their  
396 skeletal features, and in CUGW VH108 these include: the premaxilla is very small and higher  
397 than it is wide (Fig. 3C–F); the top of the maxilla is straight (in lateral views) (Fig. 3C–F); the

398 maxilla does not occupy the space of the prefrontal (in dorsal views) (Fig. 3A, B); a small  
399 portion of the maxilla extends posterior and ventral of the orbit (Fig. 3C–F); the parallelogram  
400 jugal is greater in height than width (Fig. 3C–F); the prefrontal is convex dorsally behind the  
401 naris; the parietals are bigger than the frontals (Fig. 3A, B); the middle and posterior parts of the  
402 mandible are more robust than the most anterior part in ventral view; and the angle between the  
403 two anterior edges of the entoplastron is wide ( $\sim 110^\circ$ ). It is possible that the snout of the only  
404 known specimen of *Nanhsiungchelys wuchingensis* (IVPP V3106) was deformed during the  
405 burial process, as its trumpet-shaped morphology has not been reported in any other turtles.  
406 However, the post-cranial skeleton does not show much evidence of post-mortem deformation,  
407 and both *Yeh (1966)* and *Tong & Li (2019)* regarded the unique snout as an original, diagnostic  
408 characteristic. CUGW VH108 also differs from *Nanhsiungchelys* sp. (SNHM 1558) in which the  
409 anterolateral processes are slender horn-shaped (*Hirayama et al., 2009*). Thus, CUGW VH108  
410 differs from all other known species of Nanhsiungchelyidae, and herein we erect the new species  
411 *Nanhsiungchelys yangi*.

412 The differences between *Nanhsiungchelys yangi* and *N. wuchingensis* are not likely to  
413 represent ontogenetic variation. Despite only corresponding to half of *Nanhsiungchelys*  
414 *wuchingensis* (IVPP V3106), the entire carapace length ( $\sim 55.5$  cm) of *N. yangi* (CUGW VH108)  
415 is still in the middle of the size range reported among Nanhsiungchelyidae. For instance, the  
416 entire carapace length of the Chinese nanhsiungchelyid *Jiangxichelys ganzhouensis* is  $\sim 46$ – $74$   
417 cm (*Tong et al., 2016*), and the estimated entire carapace length of adult nanhsiungchelyid  
418 *Kharakhutulia kalandadzei* is only  $\sim 23$ – $25$  cm (*Sukhanov et al., 2008*). More convincing  
419 evidence comes from the high degree of ossification of CUGW VH108, since embryonic and  
420 juvenile individuals of extant turtle usually have fontanelles on the skull roof and shells (*Gilbert*  
421 *et al., 2001*; *Sánchez-Villagra et al., 2009*). In addition, juveniles usually have a larger skull  
422 relative to their carapace, whereas mature individuals may have a relatively smaller skull  
423 (*Brinkman et al., 2013*). Furthermore, the ratios of maximum head width (HW) to straightline  
424 carapace width (SCW) are  $\sim 30\%$  in both *Nanhsiungchelys yangi* (CUGW VH108) and *N.*  
425 *wuchingensis* (IVPP V3106) (*Tong & Li, 2019*).

426 Sexual dimorphism is another possible explanation of the observed differences between  
427 *Nanhsiungchelys yangi* and *N. wuchingensis*, but this is very difficult to assess. *Cadena et al.*  
428 *(2020)* suggested that horns (similar to the anterolateral processes in *Nanhsiungchelys*) could be  
429 used to identify sex in the turtle *Stupendemys geographicus*. However, all known specimens of  
430 *Nanhsiungchelys* exhibits distinct anterolateral processes. Some extant male tortoises (e.g.  
431 *Centrochelys sulcata*) have a more robust epiplastron than females (*Zhou & Zhou, 2020*), but  
432 such a difference has not been reported in *Nanhsiungchelys*. Other lines of evidence (e.g.  
433 concavity of the plastron and shape of the xiphiplastral region) commonly used to determine the  
434 sex of extant turtles (*Pritchard, 2007*) are also unavailable due to the poor preservation of the  
435 above specimens. Based on above discussion, the most reasonable conclusion is that CUGW  
436 VH108 represents a distinct species, rather than the product of intraspecific variation.

437

### 438 **Phylogenetic position and paleobiogeography**

439 The phylogenetic analysis retrieved seven most parsimonious trees with a length of 77 steps,  
440 with a consistency index (CI) of 0.675 and retention index (RI) of 0.679. The strict consensus  
441 tree (Fig. 6) recovers *Nanhsiungchelys yangi* and *N. wuchingensis* as sister taxa, with one  
442 unambiguous synapomorphy identified: the absence of the extragulars. These two species and  
443 *Anomalochelys angulata* form a monophyletic group, which is consistent with the results of *Tong*  
444 *& Li (2019)*. Synapomorphies of this group include wide neurals, first vertebral scute with lateral  
445 edges converging anteriorly, cervical scute as wide as long, and the length to width ratio of the  
446 carapace is larger than 1.6. In particular, our new character (character 50, the length to width  
447 ratio of the carapace) supports this relationship, suggesting it could prove informative in other  
448 studies of turtle phylogeny. However, the standard bootstrap and Bremer supports values are low  
449 among these groups, and their relationships therefore need further consideration. Interestingly,  
450 our new results identify *Yuchelys nanyangensis* and *Zangerlia testudinimorpha* as sister taxa, and  
451 this relationship was supported by one unambiguous synapomorphy (their fifth vertebral almost  
452 fully covers the suprapygial).

453 Although *Anomalochelys* and *Nanhsiungchelys* were in similar stages (Fig. 6), they appear to  
454 have lived in different regions (southern China and Japan, respectively). In fact, Cretaceous turtle  
455 communities in Japan and the rest of Asia (especially China and Mongolia) are closely  
456 comparable, with both areas containing representatives of Adocusia, Lindholmemydidae,  
457 Sinochelyidae, and Sinemydidae (*Hirayama et al., 2000*). Similar extinct organisms in these  
458 regions also include the plant *Neozamites* (*Sun et al., 1993; Duan, 2005*), the bivalve  
459 *Trigonioides* (*Ma, 1994; Komatsu et al., 2007*), and the dinosaur Hadrosaurinae (*Kobayashi et*  
460 *al., 2019; Zhang et al., 2020*). *Sun & Yang (2010)* inferred that the Japan Sea did not exist during  
461 the Jurassic and Cretaceous, with the Japan archipelago still closely linked to the eastern  
462 continental margin of East Asia. This view is also supported by geological and geophysical  
463 evidence (*Kaneoka et al., 1990; Liu et al., 2017*). In addition to *Anomalochelys angulata* from  
464 Hokkaido (*Hirayama et al., 2001*), many fragments of Nanhsiungchelyidae (as *Basilemys* sp.)  
465 have also been found on Honshu and Kyushu islands, Japan (*Hirayama, 1998; Hirayama, 2002;*  
466 *Danilov & Syromyatnikova, 2008*). In China, the easternmost specimen of a nanhsiungchelyid  
467 turtle (a fragment of the shell) was recovered from the Upper Cretaceous of Laiyang, Shandong  
468 (*Li & Tong, 2017*), which is near the west coast of the Pacific Ocean and close to Japan  
469 geographically. This geographical proximity likely allowed nanhsiungchelyids to migrate  
470 between China and Japan during the Late Cretaceous.

471

### 472 **Function of the anterolateral processes of the carapace**

473 The anterolateral processes of *Nanhsiungchelys* (and *Anomalochelys*) have performed a  
474 variety of functions, but the principal function was most likely self-protection. In the earliest  
475 research on *Nanhsiungchelys wuchingensis*, *Yeh (1966)* did not discuss the function of the  
476 anterolateral processes, but speculated that the neck was flexible and the skull could be  
477 withdrawn into the shell to avoid danger. This hypothesis was supported by a complete specimen

478 (93NMBY-2) of nanhsiungchelyid *Jiangxichelys neimongolensis* whose head was withdrawn  
479 into the shell (Brinkman et al., 2015). In contrast, Hirayama et al. (2001) suggested that the large  
480 skull could not be fully withdrawn within the shell (parallel to the extant big-headed turtle  
481 *Platysternon megacephalum*) and the anterolateral processes of *Nanhsiungchelys wuchingensis*  
482 and *Anomalochelys angulata* were used for protecting the skull. Hirayama et al. (2001) also  
483 noted that *Nanhsiungchelys* has undeveloped temporal emargination, whereas *Jiangxichelys* has  
484 distinct temporal emargination, and the former condition could inhibit the ability to retract the  
485 skull inside the shell (Hirayama et al., 2009; Werneburg, 2015; Hermanson et al., 2022).  
486 Together, this suggests that despite the possession of a flexible neck that could have made it  
487 possible to retract the head, the large size of the skull and the reduced temporal emargination  
488 were considerable obstacles to doing so. Today, turtles that cannot retract the head are restricted  
489 to a few aquatic groups (e.g. Platysternidae) (Zhou & Li, 2013), whereas most turtles (including  
490 all tortoises) have this capability (Zhou & Zhou, 2020). Additional strong piece of evidence that  
491 *Nanhsiungchelys* could not retract the head is that the skulls of all known specimens (IVPP  
492 V3106, SNHM 1558, and CUGW VH108) are preserved outside of the shell, and the  
493 anterolateral processes would thus provide lateral protection for the head (Yeh, 1966; Hirayama  
494 et al., 2009; Tong & Li, 2019). Nevertheless, it seems evident that this protective strategy of  
495 *Nanhsiungchelys* was inefficient as the dorsal side of the head would be left vulnerable to attack,  
496 and this may explain why extant terrestrial turtles usually abandon this mode of protection.

497 The anterolateral processes might also have been used during fighting for mates, as  
498 hypothesized for the extinct side-necked turtle *Stupendemys geographicus* (Cadena et al., 2020).  
499 *Nanhsiungchelys* and extant tortoises share many comparable skeletal characteristics  
500 (Hutchison & Archibald, 1986) and inferred reproductive behaviors (Ke et al., 2021), and thus  
501 *Nanhsiungchelys* might have been characterized by similar combat behavior. However, all  
502 known specimens of *Nanhsiungchelys* and *Anomalochelys* possess distinct anterolateral  
503 processes, suggesting this structure might also have been present in females (although this is  
504 uncertain because it is not possible to determine their sex). If so, the anterolateral processes  
505 would not be the result of sexual dimorphism and associated combat for mates. Another piece of  
506 evidence arguing against this view is that there are no scars on the anterolateral processes of  
507 CUGW VH108, as might be expected if they were used in fighting.

508 The anterolateral processes of *Nanhsiungchelys* might also have had a secondary function in  
509 reducing drag as the animal was moving through water. Even though the Nanxiong Basin was  
510 extremely hot (~27–34 °C) during the Late Cretaceous (Yang et al., 1993), the appearance of  
511 diverse fossils of Gastropoda, Bivalvia, Charophyceae, and Ostracoda (Zhang et al., 2013)  
512 suggests the existence of lakes or rivers. Today, some tortoises living in dry areas (e.g.  
513 *Aldabrachelys gigantea* and *Centrochelys sulcata*) will immerse themselves in mud or water for  
514 a long time to avoid the hot weather (Zhou & Zhou, 2020), and *Aldabrachelys gigantea* could  
515 even swim (or float) in the ocean (Gerlach et al., 2006; Hansen et al., 2016). If *Nanhsiungchelys*  
516 had a parallel lifestyle, the anterolateral processes could have played a role in reducing resistance  
517 to fluid motion, and the efficiency of this would have been close to the level of extant freshwater

518 turtles (see Supplemental Information 3 for detailed information on hydrodynamic analyses). The  
519 reason for this is that these processes made the anterior part of the shell more streamlined (Fig.  
520 7A, B), analogous to the streamlined fairing on the anterior of airplanes and rockets. However,  
521 we acknowledge this remains a hypothesis at this time, since there is no conclusive evidence of  
522 swimming in *Nanhsiungchelys*.

523 Many of the specialized morphological features of nanhsiungchelyids (e.g. huge skull, distinct  
524 anterolateral processes, and unusually thick eggshells) are most likely adaptations to their  
525 environment. *Nanhsiungchelys* was a successful genus since it belongs to the only group of  
526 turtles that has been reported from the Dafeng Formation, suggesting these unusual turtles were  
527 well adapted to their environment. However, their specialist survival strategies might have been  
528 very inefficient because the anterolateral processes could not protect the dorsal side of the head,  
529 and the thick eggshell (Ke et al., 2021) might have hindered the breathing and hatching of young.  
530 All of these features are not present in extant turtles, suggesting this was not a dominant  
531 direction in turtle evolution. Consistent with this, nanhsiungchelyids became extinct during the  
532 Late Cretaceous, but many contemporary turtles (e.g. Adocidae, Lindholmemydidae, and  
533 Trionychidae) survived into the Cenozoic (Lichtig & Lucas, 2016).

534

## 535 Conclusions

536 A turtle skeleton (CUGW VH108) with a well-preserved skull and lower jaw, together with  
537 the anterior parts of the shell, was found in Nanxiong Basin, China. This is assigned to the genus  
538 *Nanhsiungchelys* based on the large estimated body size (~55.5 cm), the presence of a network  
539 of sculptures on the surface of the skull and shell, shallow cheek emargination and temporal  
540 emargination, deep nuchal emargination, and a pair of anterolateral processes on the carapace.  
541 Based on the character combination of a triangular-shaped snout (in dorsal view) and wide  
542 anterolateral processes, we erect a new species *Nanhsiungchelys yangi*. A phylogenetic analysis  
543 of nanhsiungchelyids places *Nanhsiungchelys yangi* and *Nanhsiungchelys wuchingensis* as sister  
544 taxa. We agree with previous suggestions that the anterolateral processes on the carapace could  
545 have protected the head, but also infer a potential secondary function for reducing drag force  
546 during movement through water. These unique characteristics might have helped  
547 nanhsiungchelyids survive in a harsh environment, but did not save them from extinction during  
548 the K-Pg event.

549

## 550 Acknowledgements

551 We thank Xing Xu (IVPP) for his useful suggestions, thank Kaifeng Wu (YSNHM) for  
552 preparing turtle skeleton, and thank Mingbo Wang (UPC), Zichuan Qin (UB), Wen Deng  
553 (CUGW) and Haoran Sun (LJU) for assistance with CFD.

554

## 555 References

556 Bell MA, Lloyd GT. 2014. strap: an R package for plotting phylogenies against stratigraphy and  
557 assessing their stratigraphic congruence. *Palaeontology* **58**:379-389. DOI:10.1111/pala.12142

- 558 **Bremer K. 1994.** Branch support and tree stability. *Cladistics* **10**:295-304. DOI:10.1111/j.1096-  
559 0031.1994.tb00179.x
- 560 **Brinkman D, Nicholls EL. 1993.** New specimen of *Basilemys praeclara* Hay and its bearing on  
561 the relationships of the Nanhsiungchelyidae (Reptilia: Testudines). *Journal of Paleontology*  
562 **67**:1027-1031. DOI:10.1017/s002233600002535x
- 563 **Brinkman D, Peng J-H. 1996.** A new species of *Zangerlia* (Testudines: Nanhsiungchelyidae)  
564 from the Upper Cretaceous redbeds at Bayan Mandahu, Inner Mongolia, and the relationships  
565 of the genus. *Canadian Journal of Earth Sciences* **33**:526-540. DOI:10.1139/e96-041
- 566 **Brinkman DB, Tong H-Y, Li H, Sun Y, Zhang J-S, Godefroit P, Zhang Z-M. 2015.** New  
567 exceptionally well-preserved specimens of “*Zangerlia*” *neimongolensis* from Bayan Mandahu,  
568 Inner Mongolia, and their taxonomic significance. *Comptes Rendus Palevol* **14**:577-587.  
569 DOI:10.1016/j.crpv.2014.12.005
- 570 **Brinkman DB, Yuan C-X, Ji Q, Li D-Q, You H-L. 2013.** A new turtle from the Xiagou  
571 Formation (Early Cretaceous) of Changma Basin, Gansu Province, P. R. China.  
572 *Palaeobiodiversity and Palaeoenvironments* **93**:367-382. DOI:10.1007/s12549-013-0113-0
- 573 **Bureau of Geology and Mineral Exploration and Development of Jiangxi Province. 2017.**  
574 *Regional geology of China, Jiangxi Province.* Beijing: Geological Publishing House. (in  
575 Chinese with English abstract)
- 576 **Cadena E-A, Scheyer TM, Carrillo-Briceño JD, Sánchez R, Aguilera-Socorro OA, Vanegas  
577 A, Pardo M, Hansen DM, Sánchez-Villagra MR. 2020.** The anatomy, paleobiology, and  
578 evolutionary relationships of the largest extinct side-necked turtle. *Science Advances*  
579 **6**:eaay4593. DOI:10.1126/sciadv.aay4593
- 580 **Danilov IG, Sukhanov VB, Syromyatnikova EV. 2013.** Redescription of *Zangerlia*  
581 *dzamynchondi* (Testudines: Nanhsiungchelyidae) from the Late Cretaceous of Mongolia, with  
582 a reassessment of the phylogenetic position and relationships of *Zangerlia*. *Morphology and*  
583 *Evolution of Turtles*, 407-417.
- 584 **Danilov IG, Syromyatnikova EV. 2008.** New materials on turtles of the family  
585 Nanhsiungchelyidae from the Cretaceous of Uzbekistan and Mongolia, with a review of the  
586 nanhsiungchelyid record in Asia. *Proceedings of the Zoological Institute RAS* **312**:3-25.
- 587 **Duan Z. 2005.** A new material of Neozamites from Yixian Formation of western Liaoning and  
588 its paleophytogeographic significance. *Global Geology* **24**:112-116. (in Chinese with English  
589 abstract)
- 590 **Gerlach J, Muir C, Richmond MD. 2006.** The first substantiated case of trans-oceanic tortoise  
591 dispersal. *Journal of Natural History* **40**:2403-2408. DOI:10.1080/00222930601058290
- 592 **Gilbert SF, Loredó GA, Brukman A, Burke AC. 2001.** Morphogenesis of the turtle shell: the  
593 development of a novel structure in tetrapod evolution. *Evolution and Development* **3**:47-58.  
594 DOI:10.1046/j.1525-142x.2001.003002047.x
- 595 **Goloboff PA, Catalano SA. 2016.** TNT version 1.5, including a full implementation of  
596 phylogenetic morphometrics. *Cladistics* **32**:221-238. DOI: 10.1111/cla.12160
- 597 **Guangdong Geological Survey Institute. 2017.** *Regional geology of Guangdong, Xianggang,*

- 598 *and Aomen (second edition)*. (in Chinese)
- 599 **Hansen DM, Austin JJ, Baxter RH, Boer EJD, Falcón W, Norder SJ, Rijdsdijk KF, Thébaud**  
600 **C, Bunbury NJ, Warren BH. 2016.** Origins of endemic island tortoises in the western Indian  
601 Ocean: a critique of the human-translocation hypothesis. *Journal of Biogeography* **44**:1430–  
602 1435. DOI:10.1111/jbi.12893
- 603 **Hermanson G, Benson RBJ, Farina BM, Ferreira GS, Langer MC, Evers SW. 2022.** Cranial  
604 ecomorphology of turtles and neck retraction as a possible trigger of ecological diversification.  
605 *Evolution*:1-21. DOI: 10.1111/evo.14629
- 606 **Hirayama R. 1998.** Fossil turtles from the Mifune Group (Late Cretaceous) of Kumamoto  
607 Prefecture, Western Japan. Report of the research on the distribution of important fossils in  
608 Kumamoto Prefecture: Dinosaurs from the Mifune Group, Kumamoto Prefecture, Japan: 85-  
609 99. (in Japanese with English abstract)
- 610 **Hirayama R. 2002.** Preliminary report of the fossil turtles from the Kitadani Formation (Early  
611 Cretaceous) of the Tetori Group of Katsuyama, Fukui Prefecture, Central Japan. *Memoir of the*  
612 *Fukui Prefectural Dinosaur Museum* **1**:29-40. (in Japanese with English abstract)
- 613 **Hirayama R, Brinkman DB, Danilov IG. 2000.** Distribution and biogeography of non-marine  
614 Cretaceous turtles. *Russian Journal of Herpetology* **7**:181–198.
- 615 **Hirayama R, Sakurai K, Chitoku T, Kawakami G, Kito N. 2001.** *Anomalochelys angulata*,  
616 an unusual land turtle of family Nanhsiungchelyidae (superfamily Trionychoidea; order  
617 Testudines) from the Upper Cretaceous of Hokkaido, North Japan. *Russian Journal of*  
618 *Herpetology* **8**:127-138.
- 619 **Hirayama R, Zhong Y, Di Y, Yonezawa T, Hasegawa M. 2009.** A new nanhsiungchelyid  
620 turtle from Late Cretaceous of Guangdong, China. In: Brinkman D, ed. *Gaffney Turtle*  
621 *Symposium*: Drumheller: Royal Tyrell Museum, 72-73.
- 622 **Hutchison JH, Archibald JD. 1986.** Diversity of turtles across the Cretaceous/Tertiary  
623 boundary in northeastern Montana. *Palaeogeography, Palaeoclimatology, Palaeoecology*  
624 **55**:1-22. DOI:10.1016/0031-0182(86)90133-1
- 625 **Jerzykiew T, Currie PJ, Eberth DA, Johnsto PA, Koste EH, Zheng J-J. 1993.** Djadokhta  
626 Formation correlative strata in Chinese Inner Mongolia: an overview of the stratigraphy,  
627 sedimentary geology, and paleontology and comparisons with the type locality in the pre-Altai  
628 Gobi. *Canadian Journal of Earth Science* **30**:2180-2195. DOI:10.1139/e93-190
- 629 **Joyce WG, Anquetin J, Cadena E-A, Claude J, Danilov IG, Evers SW, Ferreira GS, Gentry**  
630 **AD, Georgalis GL, Lyson TR, Pérez-García A, Rabi M, Sterli J, Vitek NS, Parham JF.**  
631 **2021.** A nomenclature for fossil and living turtles using phylogenetically defined clade names.  
632 *Swiss Journal of Palaeontology* **140**:1-45. DOI:10.1186/s13358-020-00211-x
- 633 **Joyce WG, Norell MA. 2005.** *Zangerlia ukhaachelys*, new species, a nanhsiungchelyid turtle  
634 from the Late Cretaceous of Ukhaa Tolgod, Mongolia. *American Museum Novitates* **3481**:1-  
635 20. DOI:10.1206/0003-0082(2005)481[0001:Zunsan]2.0.Co;2
- 636 **Kaneoka I, Notsu K, Takigami Y, Fujioka K, Sakai H. 1990.** Constraints on the evolution of  
637 the Japan Sea based on <sup>40</sup>Ar-<sup>39</sup>Ar ages and Sr isotopic ratios for volcanic rocks of the Yamato

- 638 Seamount chain in the Japan Sea. *Earth and Planetary Science Letters* **97**:211-225.  
639 DOI:10.1016/0012-821x(90)90109-b
- 640 **Ke Y, Wu R, Zelenitsky DK, Brinkman D, Hu J, Zhang S, Jiang H, Han F. 2021.** A large  
641 and unusually thick-shelled turtle egg with embryonic remains from the Upper Cretaceous of  
642 China. *Proceedings of the Royal Society B-Biological Sciences* **288**:20211239.  
643 DOI:10.1098/rspb.2021.1239
- 644 **Kobayashi Y, Nishimura T, Takasaki R, Chiba K, Fiorillo AR, Tanaka K, Chinzorig T,**  
645 **Sato T, Sakurai K. 2019.** A new hadrosaurine (Dinosauria: Hadrosauridae) from the marine  
646 deposits of the Late Cretaceous Hakobuchi Formation, Yezo Group, Japan. *Scientific reports*  
647 **9**:1-14. DOI:10.1038/s41598-019-48607-1
- 648 **Komatsu T, Jinhua C, Ugai H, Hirose K. 2007.** Notes on non-marine bivalve *Trigonioides*  
649 (*Trigonioides*?) from the mid-Cretaceous Goshoura Group, Kyushu, Japan. *Journal of Asian*  
650 *Earth Sciences* **29**:795–802. DOI:10.1016/j.jseaes.2006.06.001
- 651 **Li J, Tong H. 2017.** *Palaeovertebrata sinica, volume II, amphibians, reptilians, and avians,*  
652 *fascicle 2 (serial no. 6), parareptilians, captorhines, and testudines.* Beijing: Science Press. (in  
653 Chinese)
- 654 **Lichtig AJ, Lucas SG. 2016.** Cretaceous nonmarine turtle biostratigraphy and evolutionary  
655 events. *Cretaceous Period: Biotic Diversity and Biogeography New Mexico Museum of*  
656 *Natural History and Science Bulletin* **71**:185-194.
- 657 **Ling Q, Zhang X, Lin J. 2005.** New advance in the study of the Cretaceous and Paleogene  
658 strata of the Nanxiong Basin. *Journal of Stratigraphy* **29**:596-601. (in Chinese with English  
659 abstract)
- 660 **Liu M, Wei D, Shi Y. 2017.** Review on the opening and evolution models of the Japan sea.  
661 *Progress in Geophysics* **32**:2341-2352. (in Chinese with English abstract)
- 662 **Ma Q. 1994.** Nonmarine Cretaceous bivalve assemblages in China. *Cretaceous Research*  
663 **15**:271-284. DOI:10.1006/cres.1994.1017
- 664 **Mallon JC, Brinkman DB. 2018.** *Basilemys morrinensis*, a new species of nanhsiungchelyid  
665 turtle from the Horseshoe Canyon Formation (Upper Cretaceous) of Alberta, Canada. *Journal*  
666 *of Vertebrate Paleontology* **38**:e1431922. DOI:10.1080/02724634.2018.1431922
- 667 **Mlynarski M. 1972.** *Zangerlia testudinimorpha* n. gen., n. sp., a primitive land tortoise from the  
668 Upper Cretaceous of Mongolia. *Palaeontologia Polonica* **27**:85-92.
- 669 **Pritchard PCH. 2007.** Evolution and structure of the turtle shell. In: Wyneken J, Godfrey MH,  
670 and Bels V, eds. *Biology of turtles.* Boca Raton, FL: CRC Press, 45-84.
- 671 **Sánchez-Villagra MR, Muller H, Sheil CA, Scheyer TM, Nagashima H, Kuratani S. 2009.**  
672 Skeletal development in the Chinese soft-shelled turtle *Pelodiscus sinensis* (Testudines:  
673 Trionychidae). *Journal of Morphology* **270**:1381-1399. DOI:10.1002/jmor.10766
- 674 **Sukhanov VB. 2000.** Mesozoic turtles of Middle and Central Asia. In: Benton MJ, Shishkin MA,  
675 Unwin DM, and Kurochkin EN, eds. *The age of dinosaurs in Russia and Mongolia.*  
676 Cambridge: Cambridge University Press, 309-367.
- 677 **Sukhanov VB, Danilov IG, and Syromyatnikova EV. 2008.** The description and phylogenetic

- 678 position of a new nanhsiungchelyid turtle from the Late Cretaceous of Mongolia. *Acta*  
679 *Palaeontologica Polonica* **53**:601-614. DOI:10.4202/app.2008.0405
- 680 **Sun G, Nakazawa T, Ohana T, Kimura T. 1993.** Two *Neozamites* species (Bennettitales) from  
681 the Lower Cretaceous of Northeast China and the inner zone of Japan. *Transactions and*  
682 *proceedings of the Paleontological Society of Japan New series* **172**:264-276.
- 683 **Sun G, Yang T. 2010.** Paleontological evidence-based discussion on the origin of the Japan Sea.  
684 *Marine Sciences* **34**:89-92. (in Chinese)
- 685 **Syromyatnikova EV, Danilov IG. 2009.** New material and a revision of turtles of the genus  
686 *Adocus* (Adocidae) from the Late Cretaceous of middle Asia and Kazakhstan. *Proceedings of*  
687 *the Zoological Institute RAS* **313**:74-94.
- 688 **Tong H, Li L. 2019.** A revision of the holotype of *Nanhsiungchelys wuchingensis*, Ye, 1966  
689 (Testudines: Cryptodira: Trionychoidea: Nanhsiungchelyidae). *Cretaceous Research* **95**:151-  
690 163. DOI:10.1016/j.cretres.2018.11.003
- 691 **Tong H, Li L, Jie C, Yi L. 2016.** New material of *Jiangxichelys ganzhouensis* Tong & Mo,  
692 (Testudines: Cryptodira: Nanhsiungchelyidae) and its phylogenetic and palaeogeographical  
693 implications. *Geological Magazine* **154**:456-464. DOI:10.1017/s0016756816000108
- 694 **Tong H, Mo J. 2010.** *Jiangxichelys*, a new nanhsiungchelyid turtle from the Late Cretaceous of  
695 Ganzhou, Jiangxi Province, China. *Geological Magazine* **147**:981-986.  
696 DOI:10.1017/s0016756810000671
- 697 **Tong H, Xu L, Buffetaut E, Zhang X, Jia S. 2012.** A new nanhsiungchelyid turtle from the  
698 Late Cretaceous of Neixiang, Henan Province, China. *Annales de Paléontologie* **98**:303-314.  
699 DOI:10.1016/j.annpal.2012.08.001
- 700 **Wang W, Liu X, Ma M, Mao X, Ji J. 2016.** Sedimentary environment of Cretaceous red beds  
701 in Nanxiong Basin, Guangdong Province. *Journal of Subtropical Resources and Environment*  
702 **11**:29-37. (in Chinese with English abstract)
- 703 **Wang Y, Li Q, Bai B, Jin X, Mao F, Meng J. 2019.** Paleogene integrative stratigraphy and  
704 timescale of China. *Science China Earth Sciences* **49**:289-314. (in Chinese)
- 705 **Werneburg I. 2015.** Neck motion in turtles and its relation to the shape of the temporal skull  
706 region. *Comptes Rendus Palevol* **14**:527-548. DOI:10.1016/j.crpv.2015.01.007
- 707 **Xi D, Sun L, Qin Z, Li G, Li G, Wan X. 2021.** Lithostratigraphic subdivision and correlation of  
708 the Cretaceous in China. *Journal of Stratigraphy* **45**:375-401. (in Chinese with English  
709 abstract)
- 710 **Xu X, Pittman M, Sullivan C, Choiniere JN, Tan Q-W, Clark JM, Norell MA, Wang S.**  
711 **2015.** The taxonomic status of the Late Cretaceous dromaeosaurid *Linheraptor exquisitus* and  
712 its implications for dromaeosaurid systematics. *Vertebrata Palasiatica* **53**:29-62.
- 713 **Yang W, Chen N, Ni S, Nan J, Wu M, Jiang J, Ye J, Feng X, Ran Y. 1993.** Carbon and  
714 oxygen isotopic composition and environmental significance of Cretaceous red-bed carbonate  
715 rocks and dinosaur eggshells. *Chinese Science Bulletin* **38**:2161-2163. (in Chinese)
- 716 **Yeh H-K. 1966.** A new Cretaceous turtle of Nanhsiung, Northern Kwangtung. *Vertebrata*  
717 *Palasiatica* **10**:191-200.

- 718 **Young C-C. 1965.** Fossil eggs from Nanhsiung, Kwangtung and Kanchou, Kiangsi. *Vertebrata*  
719 *Palasiatica* **9**:141-159. (in Chinese with English abstract)
- 720 **Zanno LE. 2010.** A taxonomic and phylogenetic re-evaluation of Therizinosauria (Dinosauria:  
721 Maniraptora). *Journal of Systematic Palaeontology* **8**:503–543.  
722 DOI:10.1080/14772019.2010.488045
- 723 **Zhang X-q, Zhang X-m, Hou M-c, Li G, Li H-m. 2013.** Lithostratigraphic subdivision of red  
724 beds in Nanxiong Basin, Guangdong, China. *Journal of Stratigraphy* **37**:441-451. (in Chinese  
725 with English abstract)
- 726 **Zhang Y-G, Wang K-B, Chen S-Q, Liu D, Xing H. 2020.** Osteological re-assessment and  
727 taxonomic revision of “*Tanius laiyangensis*” (Ornithischia: Hadrosauroidea) from the Upper  
728 Cretaceous of Shandong, China. *The Anatomical Record* **303**:790-800.  
729 DOI:10.1002/AR.24097
- 730 **Zhao Z, Wang Q, Zhang S. 2015.** *Palaeovertebrata Sinica, Volume II, Amphibians, Reptilians,*  
731 *and Avians, Fascicle 7 (Serial no.11), Dinosaur Eggs.* Beijing: Science Press. (in Chinese)
- 732 **Zhao Z, Ye J, Li H, Zhao Z, Yan Z. 1991.** Extinction of dinosaurs at Cretaceous-Tertiary  
733 boundary in Nanxiong Basin, Guangdong Province. *Vertebrata Palasiatica* **29**:1-12. (in  
734 Chinese)
- 735 **Zhou T, Li P. 2013.** *Primary color illustrated handbook of classification of Chinese turtles.*  
736 Beijing: China Agriculture Press. (in Chinese)
- 737 **Zhou T, Zhou F. 2020.** *Tortoises of the World.* Beijing: China Agriculture Press. (in Chinese)  
738

# Figure 1

Geological map of Nanxiong Basin and stratigraphic distribution of valid nanhsiungchelyid turtles in China.

(A) Geological map of Nanxiong Basin, and the red triangular indicates fossil site, after Wang et al. (2016), Wang et al. (2019) and Xi et al. (2021). (B) Stratigraphic distribution of valid nanhsiungchelyid turtles in China. Abbreviations: Cam, Campanian; Cen, Cenomanian; Con, Coniacian; Maa, Maastrichtian; San, Santonian; Tur, Turonian. Stratigraphic information based on work by the Bureau of Geology and Mineral Exploration and Development of Jiangxi Province (2017) , Guangdong Geological Survey Institute (2017) , Jerzykiew et al. (1993) , Xi et al. (2021) , and Xu et al. (2015) .

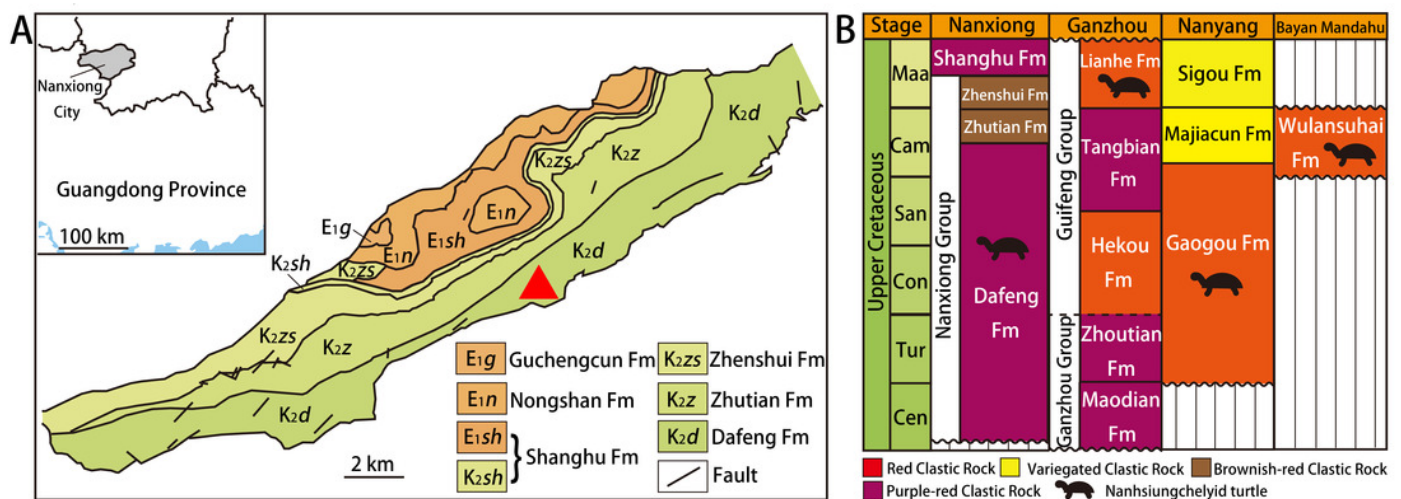


## Figure 2

Photograph (A) and outline drawing (B) of *Nanhsiungchelys yangi* (CUGW VH108) in anterior view.

Gray and black parts indicate the surrounding rock and openings of the skull, respectively. Scale bar equals 5 cm. Abbreviations: ca, carapace; md, mandible; pl, plastron; sk, skull.

A



B

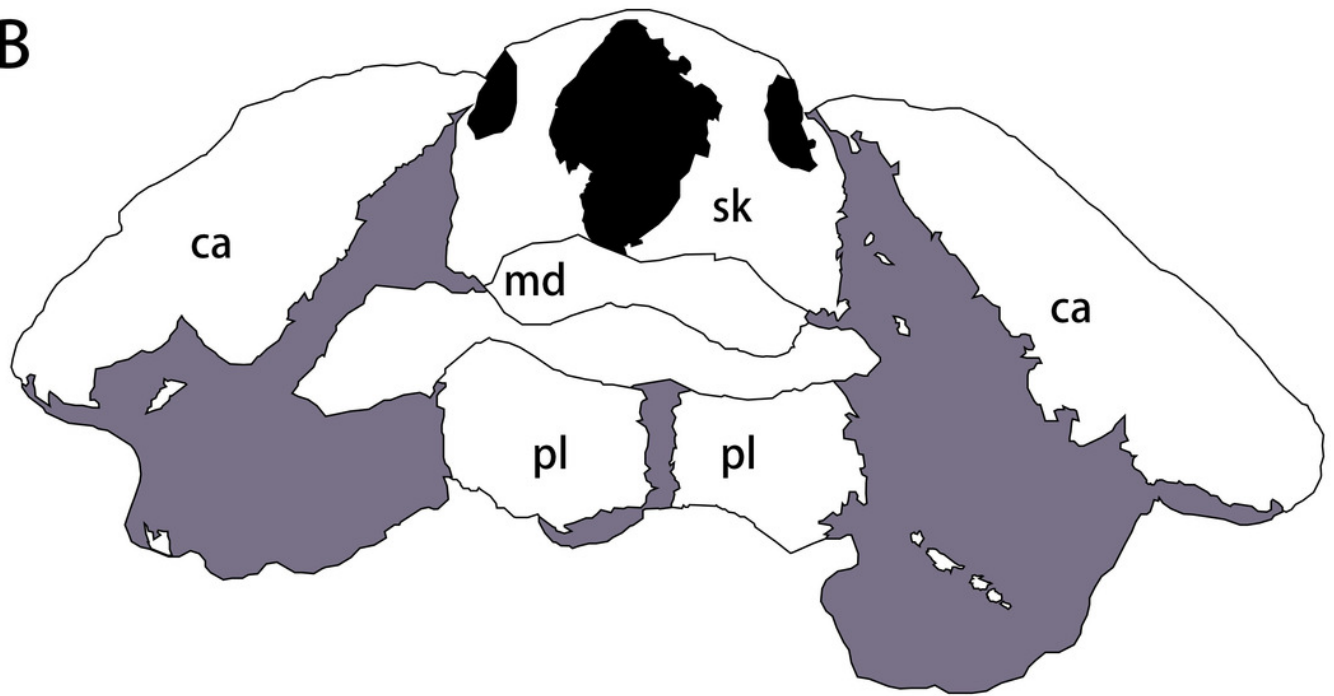


## Figure 3

The skull and carapace of *Nanhsiungchelys yangi* (CUGW VH108).

(A, B) Photograph and outline drawing of the skull and carapace in dorsal view, with a magnified view showing a distinct protrusion at the tip of anterolateral process (perpendicular to the surface of the carapace). (C, D) Photograph and outline drawing of the skull in left lateral view. (E, F) Photograph and outline drawing of the skull in right lateral view. Gray and black parts indicate the surrounding rock and openings of the skull, respectively. Scale bars equal 5 cm. Abbreviations: ca, carapace; fr, frontal; ju, jugal; md, mandible; mx, maxilla; pa, parietal; pf, prefrontal; pm, premaxilla; po, postorbital; Pr, protrusion; qj, quadratojugal.

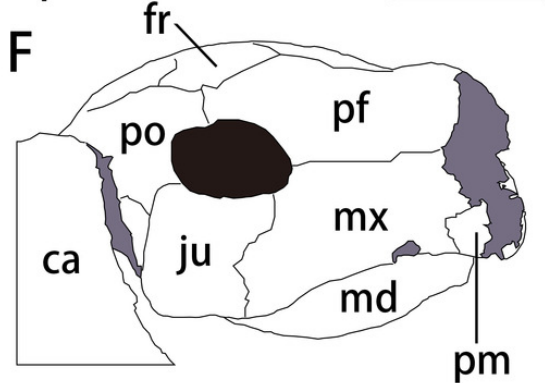
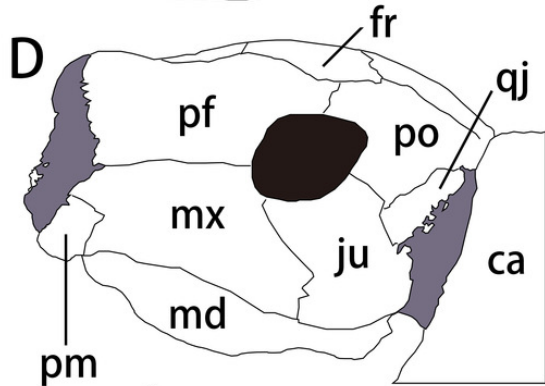
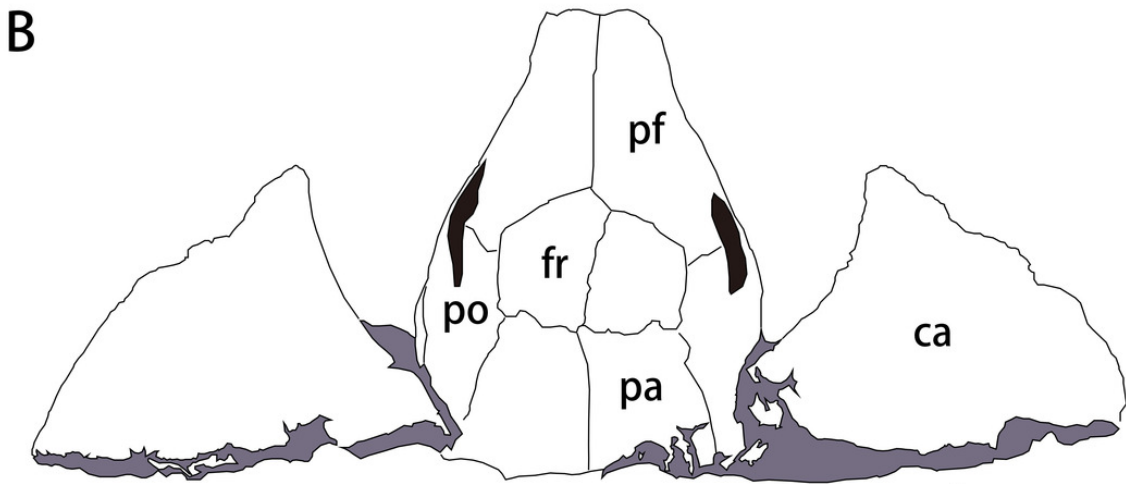
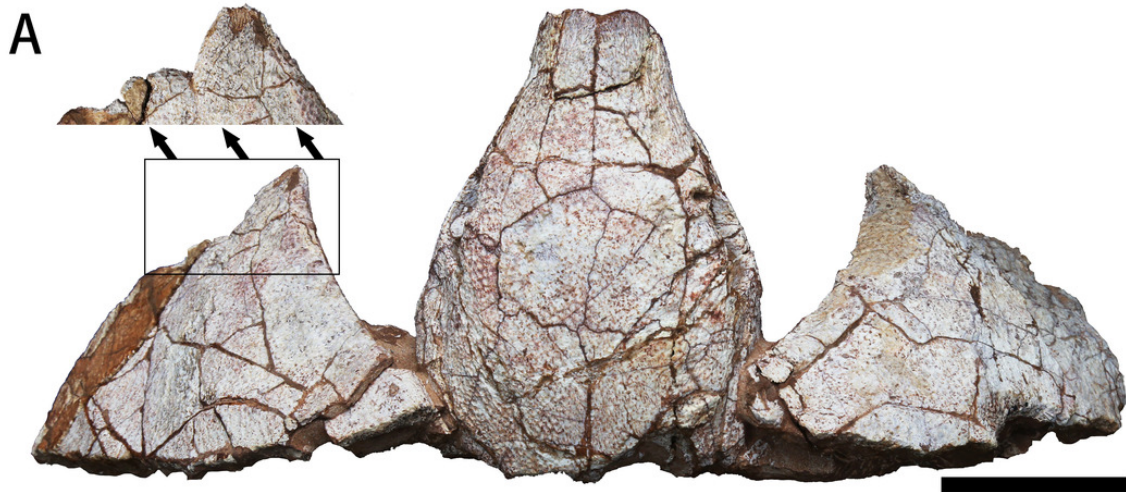


## Figure 4

Photograph (A) and outline drawing (B) of *Nanhsiungchelys yangi* (CUGW VH108) in ventral view.

Bold lines represent the sulci between scutes and gray parts indicate the surrounding rock. Scale bar equals 5 cm. Abbreviations: ca, carapace; epi, epiplastron; ent, entoplastron; Gu, gular scute; Hum, humeral scute; md, mandible; sk, skull.

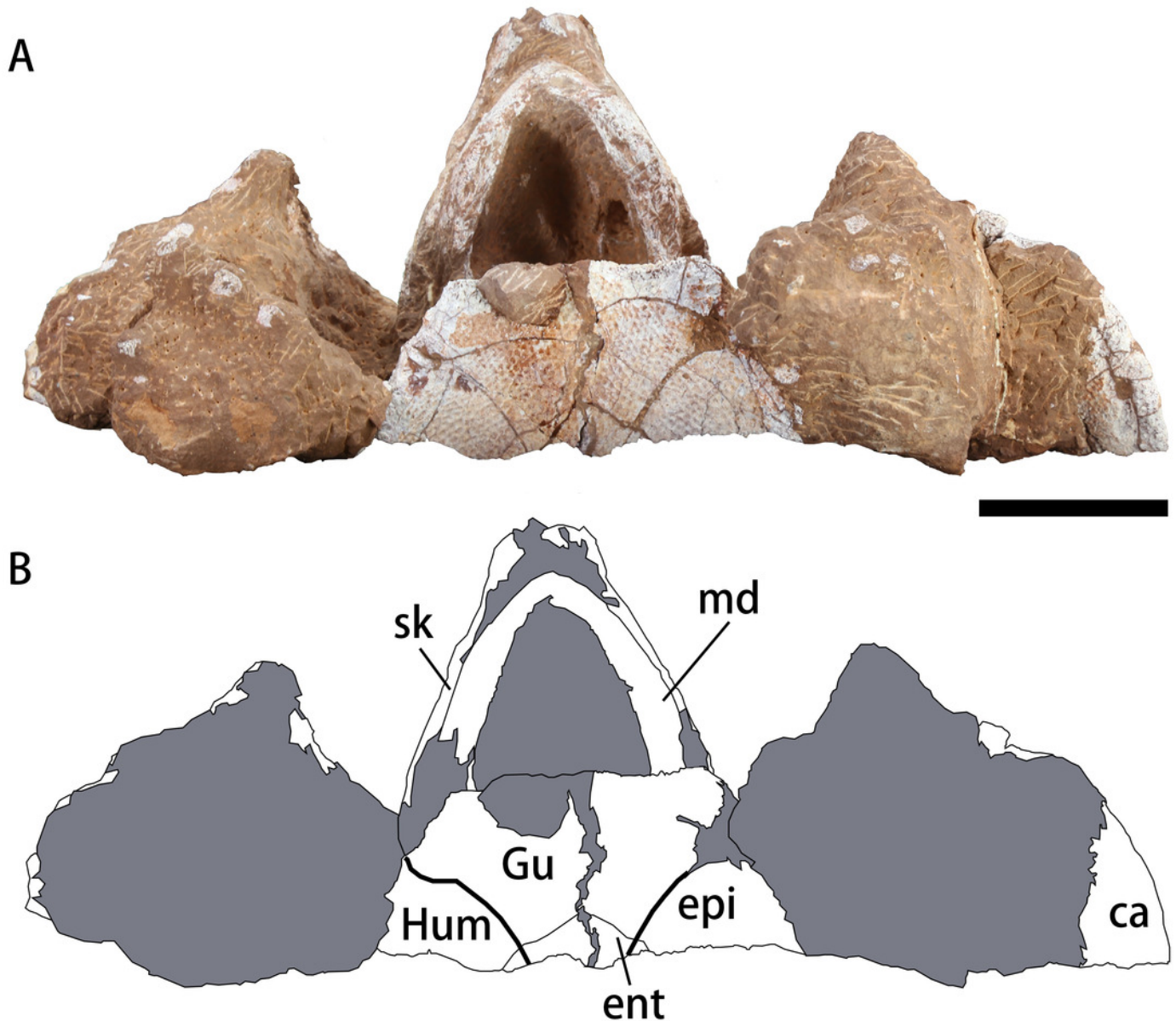


## Figure 5

Outline drawings of three nanhsiungchelyids.

(A) Skull and carapace of *Nanhsiungchelys wuchingensis*, after Tong & Li (2019) and Hirayama et al. (2001). (B) Carapace of *Anomalochelys angulata*, after Hirayama et al. (2001). (C) Skull and partial carapace of *Nanhsiungchelys yangi* (CUGW VH108). (D) Skull of *Nanhsiungchelys wuchingensis* in left lateral view, after Tong & Li (2019); arrows indicate the concave prefrontal. (E) Skull of *Nanhsiungchelys yangi* (CUGW VH108) in left lateral view. Scale bars equal 10 cm. Bold black lines represent the sulci between scutes, thin gray lines indicate the sutures between bones, and dashed lines indicate a reconstruction of poorly preserved areas. Abbreviations: bones: art, articular; Bif, bifurcation; co, costal; den, dentary; fr, frontal; ju, jugal; mx, maxilla; md, mandible; n, neural; nu, nuchal; p, peripheral; pa, parietal; pf, prefrontal; pm, premaxilla; po, postorbital; Pro, protrusion; qj, quadratojugal; sq, squamosal; scutes: M, marginal scute; P, pleural scute; V, vertebral scute; measurement: ECL, entire carapace length; MHW, maximum head width; SCW, straightline carapace width.

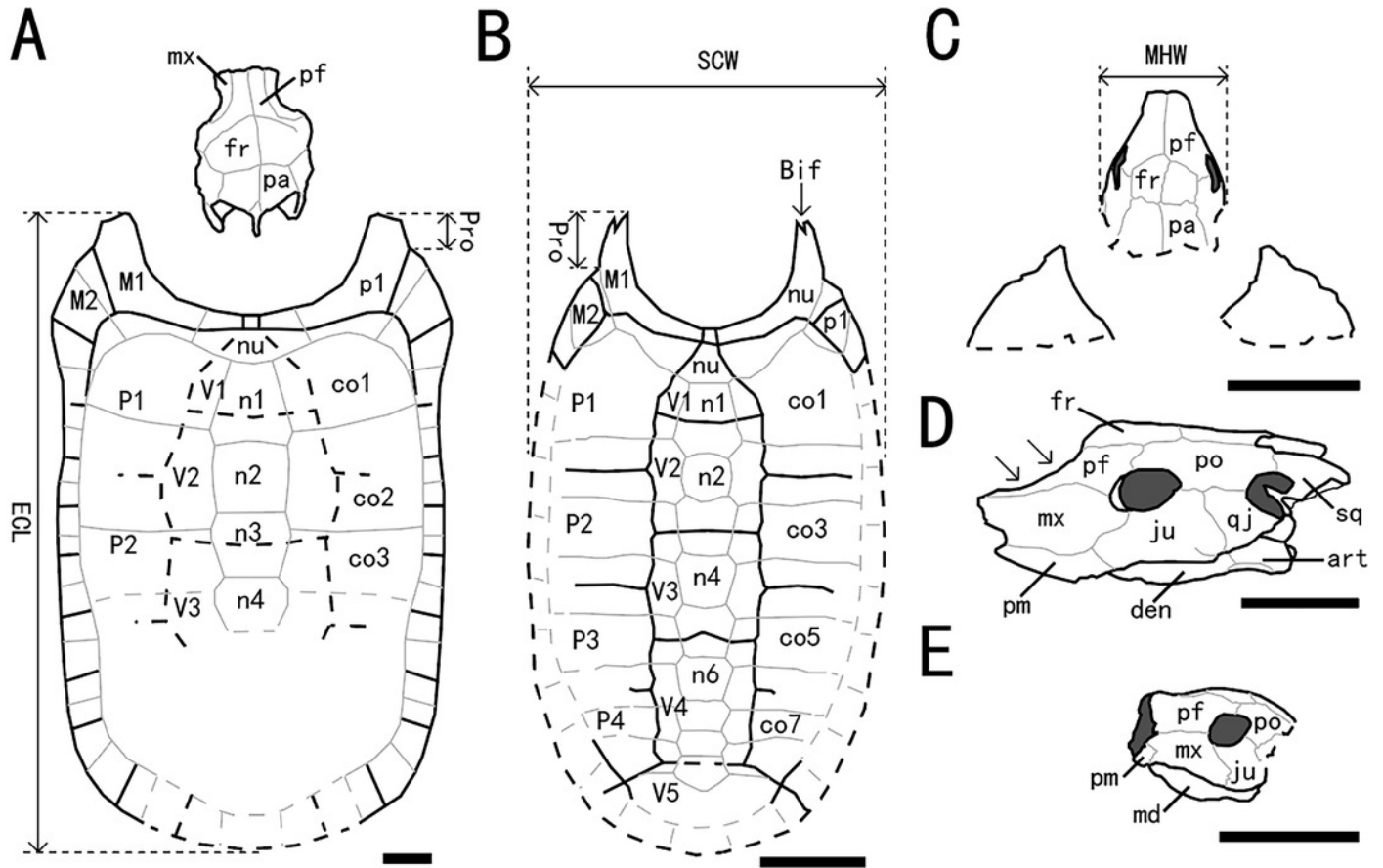


## Figure 6

Time-scaled strict consensus tree of Nanhsiungchelyidae.

Numbers above nodes are bootstrap support values and numbers below nodes are Bremer support values. Please note that the bootstrap support values less than 50 and the Bremer support values equal to 1 are not shown here. Temporal distributions of species based on Danilov et al. (2013), Li & Tong (2017), Syromyatnikova & Danilov (2009), Tong et al. (2016), Mallon & Brinkman (2018), and Xi et al. (2021). Abbreviations: Hau, Hauterivian; Barr, Barremian; Apt, Aptian; Alb, Albian; Cen, Cenomanian; Tur, Turonian; Con, Coniacian; San, Santonian; Cam, Campanian; Maa, Maastrichtian; Dan, Danian; Sel, Selandian; Tha, Thanetian; Ypr, Ypresian; Lut, Lutetian; Bar, Bartonian; Pri, Priabonian; Rup, Rupelian; Cha, Chattian; Aqu, Aquitanian; Bur, Burdigalian.

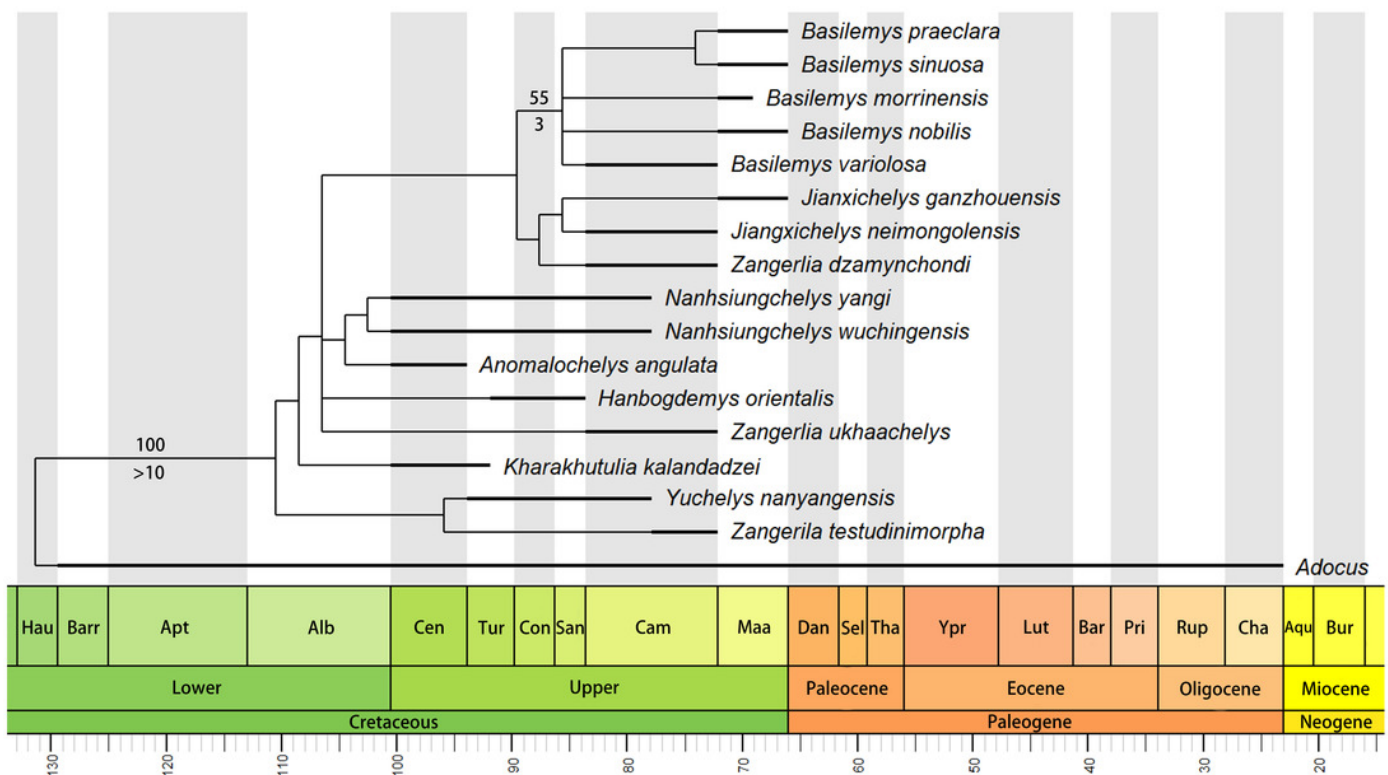


## Figure 7

3-D plots of streamlines at flow velocities of  $1.0 \text{ m s}^{-1}$ .

(A) and (B) are the model of *Nanhsiungchelys yangi* (in left lateral and dorsal views, respectively); (C) and (D) are the model of hypothetical turtle I (in left lateral and dorsal views, respectively), whose anterior carapace and body are blunt; (E) and (F) are the model of hypothetical turtle II (in left lateral and dorsal views, respectively), whose anterior carapace is streamlined and similar to most freshwater turtles. The arrows indicate the anterolateral processes. The direction of ambient flow is from left to right.

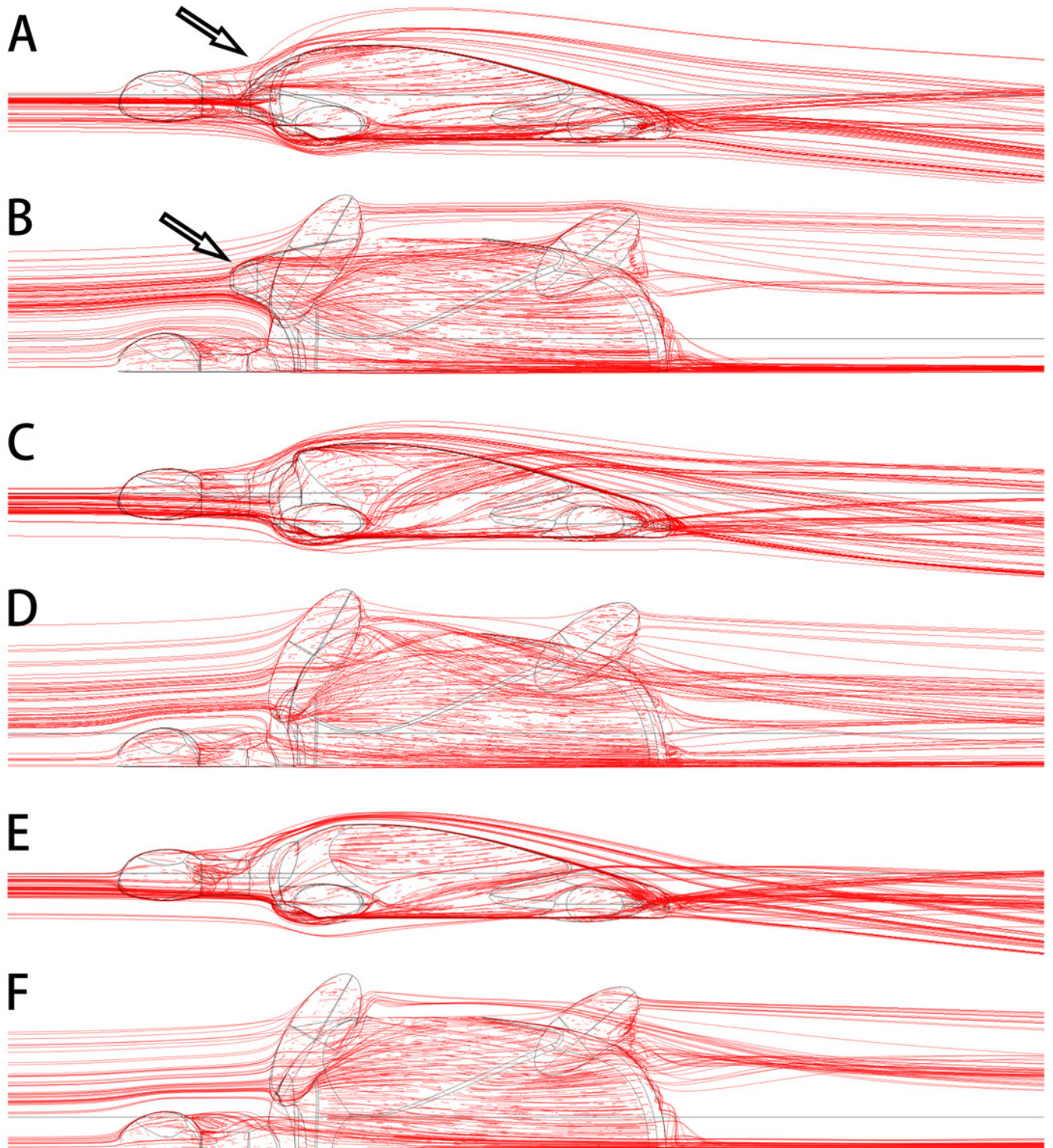


**Table 1** (on next page)

Taxonomy and distribution of Nanhsiungchelyidae in China

- 1 Table 1:
- 2 Taxonomy and distribution of Nanhsiungchelyidae in China

Taxa	Specimen Number	Location	Age	Stratigraphic Unit	References
<i>Nanhsiungchelys wuchingensis</i>	IVPP V3106	Nanxiong, Guangdong	Late Cretaceous (Cenomanian–middle Campanian)	Dafeng Formation	<i>Yeh (1966)</i> <i>Tong &amp; Li (2019)</i>
<i>Nanhsiungchelys</i> sp.	SNHM 1558	Nanxiong, Guangdong	Late Cretaceous (Cenomanian–middle Maastrichtian)	Nanxiong Group	<i>Hirayama et al. (2009)</i> <i>Li &amp; Tong (2017)</i>
<i>Nanhsiungchelys yangi</i> sp. nov.	CUGW VH108	Nanxiong, Guangdong	Late Cretaceous (Cenomanian–middle Campanian)	Dafeng Formation	This paper
<i>Jiangxichelys neimongolensis</i>	IVPP RV96007, IVPP RV96008, IVPP 290690-6 RV 96009, IVPP 020790-4 RV 96010, IVPP 130790-1 RV 96011, IMM 4252, IMM 2802, IMM 96NMBY-I-14, IMM 93NMBY-2	Bayan Mandahu, Inner Mongolia	Late Cretaceous (Campanian)	Wulansuhai Formation	<i>Brinkman &amp; Peng (1996)</i> <i>Brinkman et al. (2015)</i> <i>Li &amp; Tong (2017)</i>
<i>Jiangxichelys ganzhouensis</i>	NHMG 010415, JXGZ(2012)-178, JXGZ(2012)-179, JXGZ(2012)-180, JXGZ(2012)-182	Ganzhou, Jiangxi	Late Cretaceous (Maastrichtian)	Lianhe Formation	<i>Tong &amp; Mo (2010)</i> <i>Tong et al. (2016)</i>
<i>Yuchelys nanyangensis</i>	HGM NR09-11-14, CUGW EH051	Nanyang, Henan	Late Cretaceous (Turonian–middle Campanian)	Gaogou Formation	<i>Tong et al. (2012)</i> <i>Ke et al. (2021)</i>

3  
4

**Table 2** (on next page)

Main differences among the three species of *Nanhsiungchelys*

## 1 Table 2:

2 Main differences among the three species of *Nanhsiungchelys*

Character	<i>Nanhsiungchelys yangi</i> sp. nov.	<i>N. wuchingensis</i>	<i>N. sp.</i> (SNHM 1558)
Snout	triangular (in dorsal view)	trumpet shaped	unknown
Premaxilla	higher than wide	wider than high in lateral view and has an inverse Y-shape in ventral view	unknown
Maxilla	unseen in dorsal views; a small portion of the maxilla extends posterior and ventral of the orbit	visible in dorsal views; the maxilla is located entirely anterior to the orbit	unknown
Jugal	higher than wide	wider than high	unknown
Prefrontal	convex dorsally behind the naris	concave behind the naris	unknown
Parietal	bigger than the frontal	smaller than the frontal	unknown
Mandible	the middle and posterior parts of the mandible are more robust than the most anterior part in ventral view	nearly all parts of the mandible are equal in width	unknown
Entoplastron	the angle between the two anterior edges of the entoplastron is wide (~110°)	the angle between the two anterior edges of the entoplastron is only ~100°	unknown
Anterolateral processes	wide	wide	slender